



Feasibility Study of R-Mode using MF DGPS Transmissions

Issue: 1.0
Issue Status: Final
Issue Date: 11/03/2014]

Lead Authors: Dr. Gregory Johnson, Dr. Peter Swaszek

Prepared For: German Federal Waterways and Shipping Administration,
Federal Waterways and Shipping Agency, Northern Region
Office
Jan-Hendrik Oltmann, Michael Hoppe

This report is part-financed by the EU Regional Development Fund.



Table of Contents

Executive Summary	5
1 Introduction	7
1.1 International Context.....	8
1.2 Regional Context.....	9
2 Detailed Description of Recommended Alternatives (LP1-510)	12
2.1 Detailed Description of Agreed Upon Alternatives (LP1-310).....	16
2.1.1 L1 – Optimum Existing Case.....	16
2.1.2 L2 – Narrow Aiding Channel.....	23
2.1.3 L3 – Combination.....	26
2.1.4 L4 – Wide Aiding Channel.....	26
2.1.5 Pros/Cons of Solutions.....	27
2.2 Elaboration of Requirements for Time Synchronization (LP1-320).....	27
2.2.1 Time stability.....	27
2.2.2 Time synchronization.....	28
2.3 Performance Factors (LPI-330).....	29
2.3.1 Time signal.....	29
2.3.2 Time synchronization.....	29
2.3.3 Sky wave.....	29
2.3.4 Propagation conditions.....	33
2.3.5 Interference in 300 kHz band.....	34
2.3.6 Geometry.....	34
3 Accuracy Analysis (LP1-520)	39
3.1 Timing Accuracy (LP1-340).....	39
3.2 Positioning Accuracy (LP1-350).....	39
4 System Modifications (LP1-530)	43
4.1 Reference Station Modifications (LP1-360).....	43
4.1.1 Solution L1 (200 BPS MSK).....	43
4.1.2 Solution L2 (CW).....	43
4.1.3 Solution L3 (Combined).....	44
4.2 Beacon Receiver Modifications (LP1-370).....	45
4.2.1 Solution L1 (200 BPS MSK).....	45
4.2.2 Solution L2 (CW).....	46
4.2.3 Solution L3 (combined).....	46
4.3 Clock Specification (LP1-380).....	47
4.4 Potential Improvements (LP1-395).....	47
5 Test Bed Concept (LP1-540)	49
5.1 Development of concept for testing R-Mode in a field trial (LP1-400).....	49
5.1.1 Transmitter.....	49
5.1.2 Mobile Receiver.....	50
5.1.3 Monitor Receiver.....	50
5.2 Field test concept study (LP1-410).....	50
5.2.1 Transmitter Locations.....	51
5.3 R-mode Receiver Concept (LP1-420).....	54

6 Conclusions	55
7 References.....	56

Table of Figures

Figure 1: Daytime (left) and night time (right) predicted positioning accuracy (m) using a 0-100m scale.	6
Figure 2: Rudimentary representation of overarching e-Navigation architecture: shipboard, shore-based and links in-between [1].....	8
Figure 3: The place of the IALA e-Navigation stack and its layers within the overarching e-Navigation architecture from [1].	9
Figure 4: Ship traffic density in the NSR reprinted from [3]. The labels show the total number of ships passing each line from both directions during 2012. The red colour gradient shows the relative density of shipping in the NSR. The empty area in the middle of the North Sea is an area without AIS coverage (it does not mean that there is no traffic).....	10
Figure 5: IMO overarching e-Navigation Architecture represented as “7 Pillars”, reprinted from [3].	11
Figure 6: Building blocks mapped to solution sets and proposed solutions.	15
Figure 7: The modified CRB for estimating the time of a bit transition. At a typical SNR of 25 dB, the standard deviation would be 0.5 msec, which equates to about 150 km.	18
Figure 8: A comparison of the MCRB and achievable performance (reprint of Figure 5 from [34])......	19
Figure 9: The modified CRB for estimating the time from the phase. For the same typical 25 dB SNR, the standard deviation is ~9 nanoseconds which equates to ~2.7 meters.....	20
Figure 10: MSK Spectrum in red, CW Signals in blue, adjacent channel MSK with its own CW in green.....	23
Figure 11: A single hop sky wave.....	30
Figure 12: Typical sky wave delay versus distance.	30
Figure 13: Typical fade margin assuming smooth earth model.....	31
Figure 14: Example of sky wave interference on MSK.	32
Figure 15: Worst-case time bias as a function of the fade margin.	33
Figure 16: Frequency Reuse Distribution, compiled from IALA listings of DGNSS transmitters. The top bar, for example, indicates that there are 3 frequencies (channels) that are used 4 times each.....	34
Figure 17: HDOP for the North Sea.....	35
Figure 18: Predicted signal strengths (in dBμV) for three beacons around the North Sea.	36

Figure 19: Ground conductivity map; each level maps to one of the ITU-R ground conductivity ranges [58].....	37
Figure 20: Interpolated noise map, dB μ V/m.	38
Figure 21: Daytime Predicted Positioning Accuracy (m) using 0-100m scale.	40
Figure 22: Daytime Predicted Positioning Accuracy (m) using 0-20m scale.	40
Figure 23: Predicted Positioning Accuracy (m) at night using 0-100m scale.....	42
Figure 24: Predicted Positioning Accuracy (m) at night using 0-200m scale.....	42
Figure 25: Transmitter for Solution L1.	43
Figure 26: Transmitter for Solution L2.	44
Figure 27: Receiver for Solution L1.	45
Figure 28: Receiver for Solution L2.	46
Figure 29: Receiver for Solution L3.	47
Figure 30: Ijmuiden site (black triangle) with 200 km range ring in yellow and 100 km range ring in red.	49
Figure 31: Flexibilis DGNSS Modulator.	50
Figure 32: Test Bed HDOP for three German Stations plus Netherlands and Denmark.	51
Figure 33: Test Bed HDOP for three German Stations plus Netherlands.	52
Figure 34: Test Bed HDOP for three German Stations plus Denmark.	52
Figure 35: Test bed HDOP for three German Stations.	53
Figure 36: Test Bed HDOP for two German Stations plus Netherlands and Denmark.....	53
Figure 37: All-in-view R-Mode receiver.....	54
Figure 38: North Sea Area HDOP with the addition of the Ekofisk station (circled).....	55

List of Tables

Table 1: The 17 Identified Building Blocks.....	12
Table 2: Accuracy and Lane Resolution.....	25
Table 3: Pro's and Con's of Three Solutions.	27
Table 4: Conductivity Map Levels and Descriptions.	37
Table 5: Annual average noise values not exceeded 95% of the time, in dB μ V/m, reprinted from [59].	38

Executive Summary

High precision positioning in the maritime domain is now the norm since the introduction of Global Navigation Satellite Systems (GNSS). Unfortunately, it is well known that as low power, satellite-based systems, GNSS are vulnerable to interference (both naturally occurring and manmade); hence, the development of an alternative backup system is recommended. A variety of technological solutions to this backup requirement are possible; in the radio frequency (RF) domain we have the so-called “Signals of Opportunity” (SoOP) approach. Of interest to this study is the use of the Differential GNSS (DGNSS) broadcasts as a SoOP. These medium frequency (MF) RF broadcasts, in the 283.5-315 kHz (Region I) marine band, currently transmit correction and integrity information for the GNSS using minimum shift keying (MSK). This report considers several DGNSS-based solutions to provide a Ranging Mode (R-Mode) Position Navigation and Timing (PNT) alternative to GNSS. This work is being done in support of the EU INTERREG IVb North Sea Region Programme project ACCSEAS (Accessibility for Shipping, Efficiency Advantages and Sustainability), which is a 3-year project supporting improved maritime access to the North Sea Region through minimising navigational risk.

The DGNSS ranging system (aka R-Mode) described in this report is directly linked to the IALA e-Navigation Architecture being both a mitigation system to GNSS failures (part of the WWRNS) and part of the CSSA as a technical service (part of the Medium Wave Broadcast Service).

DGNSS R-Mode is a backup to GNSS that can meet the resilient PNT requirements of e-Navigation.

In the Milestone 1 report, a variety of potential ideas and methods to implement R-Mode were identified; these could be described as building blocks for a full solution. Each of the building blocks was evaluated using various metrics such as technical feasibility and implementation cost and difficulty; this evaluation was detailed in the Milestone 1 report. At the Milestone 1 meeting it was agreed to group the building blocks into mutually independent solution sets. These solution sets were then combined into four potential solutions:

- L1 – Optimum Existing Case: this solution combines adding a new message and an increased data rate of 200 bps to the existing MSK signal.
- L2 – Narrow Aiding Channel: this solution consists of adding CW signal(s) to the existing MSK signal.
- L3 – Combination: this solution is a combination of L1 and L2.
- L4 – Wide Aiding Channel: this solution is similar to L2 but ignores the bandwidth constraints and could consist of, perhaps, the two-tone concept.

Each of the primary solutions (L1 – L3) is examined in some detail in this report. The analysis shows that they all can provide TOA performance bounded by:

$$\sigma_{\tau}^2 \geq \frac{1}{2\omega_c^2 T SNR}$$

In the case of L1 this is achieved using either an estimate on the phase of the carrier or on the bit transitions using a new (fixed) message. In the case of L2 and L3 this is achieved using a phase estimate on the CW signal. In all cases the cycle (lane) ambiguity must be resolved. In the case of L1 and L3 this is done using bit transition estimation on the new message. In the case of L2, this is done using the beat frequency of the two CW signals.

The recommended solution is L3, MSK with a single CW signal added. The TOA performance bound above is achieved using phase estimates on the CW signal, which is easier than phase estimates on the MSK carrier. Cycle resolution is achieved using bit

transitions on the new message (but only needed periodically, not continuously, so the MSK data channel throughput is preserved).

The ranging performance is impacted by a variety of factors that are explored in this report: time stability and synchronization, self-channel sky wave interference, ground wave propagation variances, co-channel interference (other DGNSS broadcast on the same frequency), and geometry. In the position analysis it is assumed that the time stability (on the order of 1 ns) and synchronization (to within 50-100ns) to a common reference such as UTC is achievable. Sky waves can have a large impact on ranging performance at night so separate results are presented for day and for night. Propagation variances and co-channel interference are assumed to have minimal impact. The geometry of the position solution, as measured by the Horizontal Dilution of Precision (HDOP), is a major factor in overall positioning performance, but HDOP values in the North Sea Area are quite good (generally less than 2).

The predicted daytime bound on R-Mode positioning using TOA accuracy bounds is very good – better than 10m accuracy in most of the North Sea Area. The nighttime R-Mode performance is about a factor of 10 worse than daytime performance, but still better than 100m accuracy for most of the North Sea Area (see Figure 1). Several other ideas for future improvements are presented.

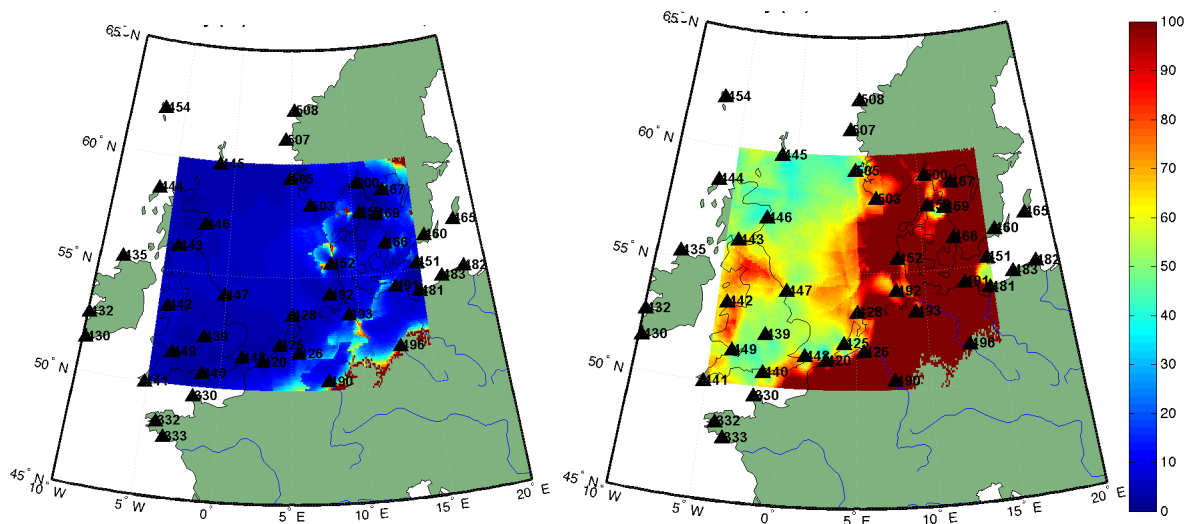


Figure 1: Daytime (left) and night time (right) predicted positioning accuracy (m) using a 0-100m scale.

This report identifies the system modifications (both transmitter and receiver) that would be necessary to implement a test of R-Mode. Conceptual test beds for both near-term (ACCSEAS) and medium-term (future German test bed) are also described. Finally the architecture for a future all-in-view R-Mode receiver is presented.

1 Introduction

High precision positioning in the maritime domain is now the norm since the introduction of Global Navigation Satellite Systems (GNSS). Unfortunately, it is well known that as low power, satellite-based systems, GNSS are vulnerable to interference (both naturally occurring and manmade); hence, the development of an alternative backup system is recommended.

A variety of technological solutions to this backup requirement are possible; in the radio frequency (RF) domain we have the so-called “Signals of Opportunity” (SoOP) approach. This term refers to the opportunistic use of RF signals, typically communications signals, which exist in the geographical area of the receiver. While these signals are not primarily intended for positioning, a SoOP navigation receiver attempts to exploit them as such. Specifically, if each SoOP can provide a (pseudo-) range to the receiver from a known location, a trilateration position solution is possible. Even if a complete position solution is impossible from the SoOP (perhaps due to too few signals being present), the resulting pseudorange information could be combined with measurements from existing positioning systems in a position solution (e.g. combining with eLoran or perhaps with GNSS measurements limited by urban canyons).

Of interest to this study is the use of the Differential GNSS (DGNSS) broadcasts as a SoOP. These medium frequency (MF) RF broadcasts, in the 283.5-315 kHz (Region I) marine band, currently transmit correction and integrity information for the GNSS using minimum shift keying (MSK). MSK is a narrowband, continuous phase, constant amplitude, binary communications method. As implemented for DGNSS, the data rates are typically 100 or 200 bps.

As a SoOP, the DGNSS signal has several advantages:

- Good geographical coverage of the stations – the transmitters are not in the centers of populated areas; rather, they are evenly dispersed along coastlines and waterways.
- DGNSS transmitters are typically under government control; hence, availability and continuity are high.
- The DGNSS transmit antennas are omni-directional and their locations can be surveyed.
- The DGNSS signal primarily travels as a ground wave with good building penetration.
- The MSK signal has two natural signal parameters (time of bit transition and carrier phase) that could easily be time-synchronized at the transmitter. This synchronization eliminates the need for a monitor station; hence, simplifying implementation of the infrastructure for a positioning system. Without such synchronization, the DGNSS broadcast could itself accommodate the data bandwidth for disseminating monitor timing information.

As a disadvantage, a DGNSS SoOP is susceptible to multipath interference due to signal reflection off of the ionosphere (sky wave). It is expected that this will limit the coverage range of individual transmitters.

This report considers several DGNSS-based solutions to provide a Ranging Mode (R-Mode) Position Navigation and Timing (PNT) alternative to GNSS.

1.1 International Context

As defined by the International Maritime Organization (IMO):

e-Navigation is the harmonised collection, integration, exchange, presentation and analysis of maritime information onboard and ashore by electronic means to enhance berth to berth navigation and related services, for safety and security at sea and protection of the marine environment. – IMO (MSC 85) definition of e-Navigation

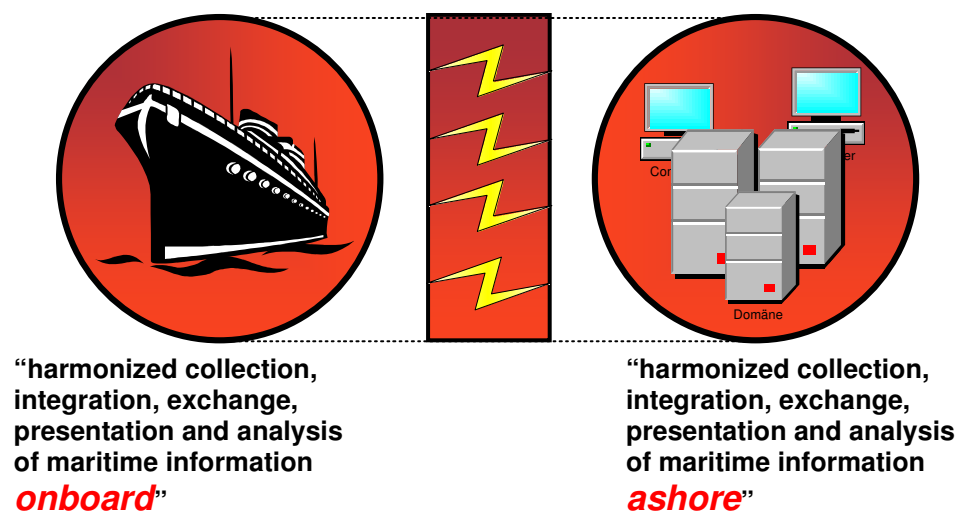


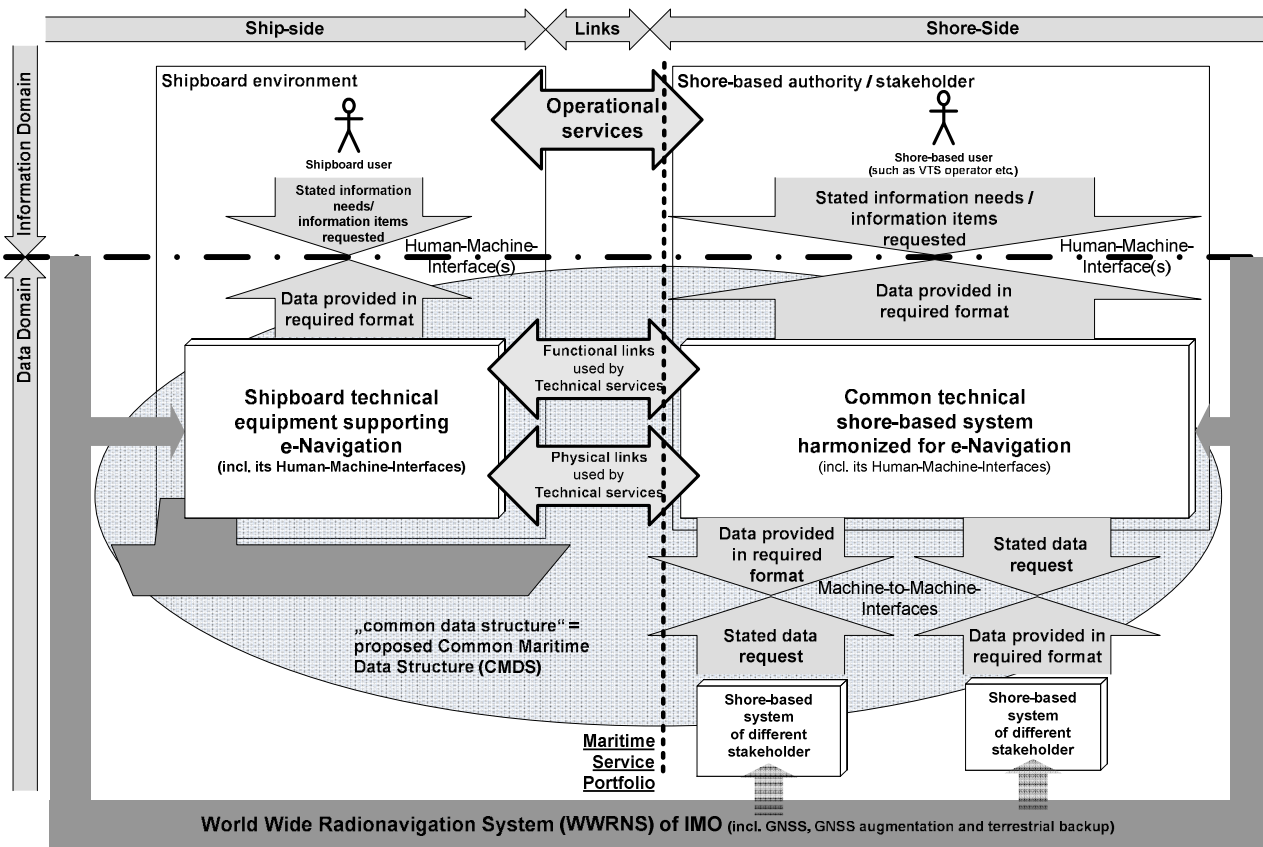
Figure 2: Rudimentary representation of overarching e-Navigation architecture: shipboard, shore-based and links in-between [1]

A graphical view of this definition is shown in Figure 2, reprinted from the draft revision to IALA e-NAV-140 [1]. This same document goes on to describe in more depth the proposed e-Navigation architecture to implement the IMO vision and also introduces the concept of the e-Navigation stack. These two concepts are shown in Figure 3 (also from [1]). In this figure, the dashed vertical line represents the boundary of the Maritime Service Portfolio (MSP) which “defines and describes a set of operational and technical services and their level of service provided by a stakeholder in a given sea area, waterway, or port, as appropriate. Mainly, the services and MSPs are provided from a-shore or shore-based. MSPs should be developed to achieve harmonization, modernization, integration and simplification on board and ashore, taking into account the use of the IHO’s S-100 standard” [1]. The red-outlined box contains the Common Shore-based System Architecture (CSSA) which is described in the draft IALA Recommendation on the Common Shore-based System Architecture [2].

“As indicated in Figure 3, there is a dependency of the e-Navigation architecture on external systems such as GNSS, augmentation, and backup systems for position fixing and for timing. This may pose certain vulnerability for all e-Navigation applications, since dynamic position information is involved in most and time information is required in each one. Hence, mitigation methods are important.

GNSS signals are monitored by augmentation systems whose use is twofold. They improve the accuracy of GNSS positioning in accordance with the requirements for different phases of berth-to-berth navigation (ocean, coastal, harbour approach, canal/river, docking). But augmentation systems also inform the user by means of integrity information, if the system can be used for a specific application. A prominent example for a shore-based augmentation system is the IALA radio beacon DGNSS which can be considered as a technical e-Navigation service within the CSSA.

In case of GNSS failure, the e-Navigation architecture takes into account terrestrial backup systems that are an independent source of positioning and timing information. However, it has to be ensured that the terrestrial navigation systems can fulfil the required performance (e.g., accuracy, integrity, continuity)."[1]



Note: There are operational and technical interactions between different shipboard environments. These are not shown for simplicity's sake in this figure.

Figure 3: The overarching e-Navigation architecture from [1].

The DGNSS ranging system (aka R-Mode) described in this report is thus directly linked to the IALA e-Navigation Architecture being both a mitigation system to GNSS failures (part of the WWRNS) and part of the CSSA as a technical service (part of the Medium Wave Broadcast Service).

1.2 Regional Context

This work is being done in support of the EU INTERREG IVb North Sea Region Programme project ACCSEAS (Accessibility for Shipping, Efficiency Advantages and Sustainability), which is a 3-year project supporting improved maritime access to the North Sea Region through minimising navigational risk. The goals of the ACCSEAS project are to¹:

- identify key areas of shipping congestion and limitation of access to ports;
- define solutions by prototyping and demonstrating success in an e-Navigation test-bed at North Sea regional level.

¹ From <http://www.accseas.eu/about-accseas>.

The North Sea Region (NSR) as defined by ACCSEAS [3] includes the eastern part of UK, Belgium, the Netherlands, the northern part of Germany, Denmark, the southern part of Norway, and the western part of Sweden as well as the Skagerrak and Kattegat, the Sounds and the south-western part of the Baltic Sea. The three largest and busiest ports in the NSR are Rotterdam, Antwerp, and Hamburg. This area is shown in Figure 4 with ship traffic densities in red. Based on the traffic and risk analysis done using the IALA IWRAP model, about 70% of the predicted collisions take place north of Germany and the Netherlands, making this a key area for testing and implementation of R-Mode.

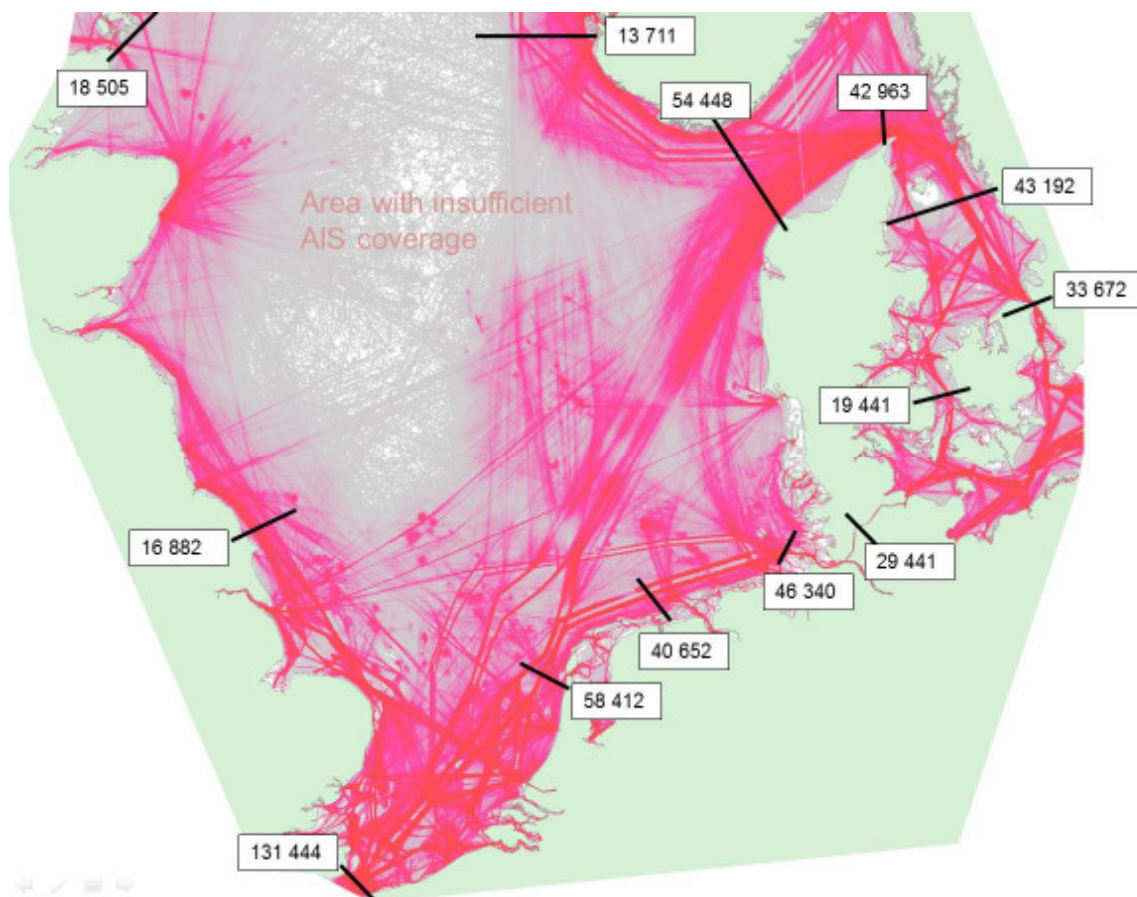


Figure 4: Ship traffic density in the NSR reprinted from [3]. The labels show the total number of ships passing each line from both directions during 2012. The red colour gradient shows the relative density of shipping in the NSR. The empty area in the middle of the North Sea is an area without AIS coverage (it does not mean that there is no traffic).

The recently released “Baselines and Priorities Report” [3] contains an analysis of the traffic in the region, both current and projected. The planned enormous expansion of wind farms will reduce the navigable space and could impact key shipping lanes, raising safety and efficiency concerns. The report also traces user needs to system requirements using a system engineering approach. One of the low Level User Requirements identified was the need for resilient PNT.

The ACCSEAS project activities are aligned with the IMO e-Navigation concept as shown in Figure 3. This can also be visualized as the so-called “7 Pillars of e-Navigation” as shown in Figure 5. The pillar of interest to this report is the Resilient PNT pillar which is defined as

“Highly reliable and robust determination of Position, Navigation data and Time (PNT) at the shipboard and shore-based electronic systems with the World Wide Radio Navigation System (WWRNS) of IMO at the core” [3]. The ACCSEAS potential solution that maps to this pillar is the Multi-Source Positioning Service (MSPS). “The resilient PNT technical services - e.g. Ranging Mode (R-Mode) – that are based on backup technologies independent of GNSS could be central to the e-Navigation and test-bed architectures to meet the user need for resilient PNT. These technical services could support a MSPS operational service that would provide, monitor and distribute resilient PNT information to a broad range of e-Navigation operational services” [3].

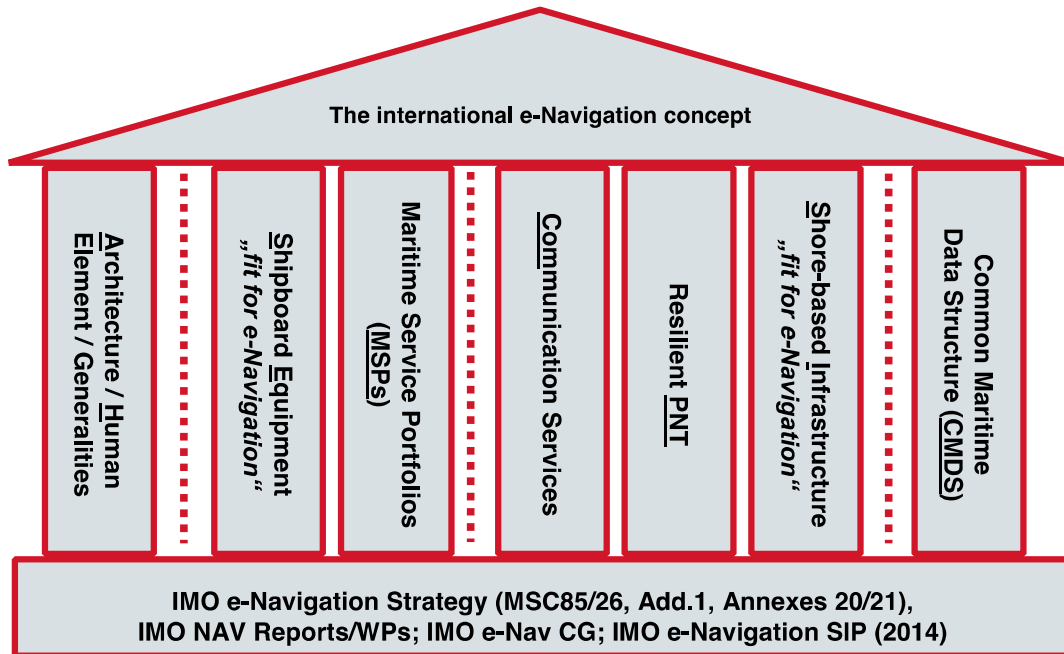


Figure 5: IMO overarching e-Navigation Architecture represented as “7 Pillars”, reprinted from [3].

DGNSS R-Mode is a backup to GNSS that can meet the resilient PNT requirements of e-Navigation

2 Detailed Description of Recommended Alternatives (LP1-510)

In the Milestone 1 report, a variety of potential methods to implement R-Mode were identified. These methods were based on current and previous work by the authors [4-7] and others as presented in the open literature [8-14]. These ideas could be described as building blocks for solutions. The proposed methods were separated into three broad categories: (A) no significant transmitter hardware change, (B) modifications to the current transmission, but staying within the existing bandwidth channel assignment, and (C) broader changes to the transmission. The proposed methods were numbered sequentially within the three categories (no significance to the order within the categories). These 17 building blocks are listed in Table 1.

Table 1: The 17 Identified Building Blocks.

#	Rmode Option	Description
A1	Use existing MSK signal as is	Based upon the existing signal specification and the results reported in [6], the receiver would estimate both the times of bit transition and the carrier phases of all DGNSS signals present (in the literature, this is called an “all-in-view” receiver). While the receiver might limit its attention to the message preamble so as to eliminate the effect of the randomness of the message on the estimation performance, this is likely to be too small a data window for good performance.
A2a	Use existing signal with a longer (redesigned) preamble on each message	Using a longer (known) preamble on each message is considered.
A2b	Use existing MSK signal with new RTCM message type	The advantage is that a known data sequence helps in the pseudo-range estimation and should improve on our prior estimates of performance in [6] which were dependent upon a random data model.
A3	Directional receiver antenna to reduce skywave	Assuming a flat earth model, a skywave from a station at a distance of 100 km is coming in at approximately 60° above the horizon; hence, a receive antenna (some form of loop?) with a low elevation aperture could limit skywave from stations used in the position solution. While we would still suffer from stations further away (due to their lower skywave elevation), our ability to resolve close stations will be greatly increased with a horizontally directed antenna.
A4	Range and bearing from one signal	Thinking of the DGNSS transmitters as non-directional beacons, a SoOP receiver could employ both pseudo-range and bearing estimates in its positioning algorithm.
B1	Use existing MSK signal at higher bit rate	It was observed in [6] that the accuracy of the bit timing estimate is inversely proportional to the MSK data rate; hence, increasing the number of bits per second equates to better resolution on the bit edge. Unfortunately, such an increase also increases the bandwidth of the MSK signal, so the rate cannot be increased by too much and we do not expect too much gain here.
B2	Amplitude modulate the MSK signal (small BW)	Recognizing the value of amplitude variation in the cross-correlation techniques used with AM SoOPs, we might amplitude modulate the MSK signal to improve the receiver’s ability to resolve the underlying ambiguity in the sinusoidal correlation function. While this conceptually could improve matters, modulating the amplitude will also increase the bandwidth of the inherently narrowband MSK; hence, only limited modulation is possible, probably too little to provide enough gain here.

#	Rmode Option	Description
B3	Add a pulsed signal on same channel	As has been demonstrated with Loran, a pulsed signal can effectively eliminate the impact of multipath. To do the same for DGNSS ranging, yet preserve the data carrying capacity, a pulsed signal could be time multiplexed with the current MSK. Unfortunately the narrow bandwidth allocated to DGNSS (500 Hz in Europe) limits the effectiveness of this idea.
B4	Overlay an alternating 1-0 modulated signal on the same channel	The idea is to simultaneously broadcast two MSK signals at the same center frequency, the current signal at its design bit rate and a second at a higher bit rate. The proposed 1-0 alternating sequence fixes the spectrum of this second signal as narrowband and the higher rate moves the spectrum away from the current DGNSS spectrum (much as the BOC codes used in GNSS L1C to separate the spectrum away from L1). Potentially these additional signals could be put at the channel edges (± 250 Hz) on every other channel so as to minimize impact on legacy signals. A significant technical question here is the ability of the transmitter (amplifier and antenna) to effectively generate such a signal.
B5	Add a CW signal to same channel	Instead of a second MSK signal on the same channel, sinusoidal continuous-wave (CW) signals (with their correspondingly narrow spectra) could be overlaid on the MSK transmission. This would essentially be a modernized, medium frequency Decca system [15]. The SoOP receiver would exploit the phase of this signal, as described above in the AM SoOP systems. Such a system would be distinct from Decca in that it would be all-in-view.
C1a	Spread spectrum - block of adjacent channels - use CDMA, FTDMA?	The same concepts as B1 - B5, but pushed to the extreme. A somewhat wider bandwidth would allow for higher data rates, more amplitude modulation, pulsed signals, or overlays, both MSK and CW; in general, CDMA or some form of FTDMA could be considered. However, the regulatory limits on the band probably make such widening unrealistic to envision
C1b	MSK at very high bit rate (wider than 1 channel)	
C2	AM modulate MSK - wider bandwidth than 1 channel	
C3	Add a pulsed signal on a second channel	
C4	Overlay an alternating 1-0 modulated signal on a second channel	
C5	Add a CW signal to second channel	
C6	Use existing MSK signal - two-tone concept	Simultaneous transmission of two MSK signals was originally proposed in [16] to combat DGNSS fading and, hence, to extend the range of transmission. We extended the two-tone idea to ranging in [7] to remove the need for data aiding in the pseudo-range estimates. Conceptually, the system would use a single DGNSS antenna to broadcast two synchronized copies (same timing and data) of the MSK DGNSS signal at two different carrier frequencies. DSP techniques to combine the synchronous receptions could cancel out the data and create two CW signals at the sum and difference frequencies of the MSK carriers. Phase tracking of both of these low frequency (~ 3 kHz) and high frequency (~ 600 kHz) signals would provide a coarse and fine pseudo-range measurement. As this is only a conceptual statement, further analysis is needed along with the development of algorithms for the resolution of the resulting ambiguity.

Each of the building blocks in Table 1 was evaluated using the following metrics:

- Technical feasibility of the precision time signal modulated on MSK.
- Limitations of the approach such as accuracy.
- Modulation and spectrum requirements.
- Compliance with standards (data formats, radio link, transmitter and receiver technology).
- Technical and economic implementation costs for transmitter stations.

This evaluation was detailed in the Milestone 1 report. At the Milestone 1 meeting it was agreed to group the building blocks into mutually independent solution sets. These solutions sets and the building blocks that map to them are (see Figure 6):

- S1 – Modification of the Data Contents (building blocks A1, A2a, and A2b).
- S2 – Modification of the Data Rate (building blocks B1 and C1b).
- S3 – Add an Additional Data Channel, Band and Channel Spacing Compliant (building blocks B2, B4, B5, and C6).
- S4 – Direction Selection, Receiver-side Antenna Modification (building blocks A3 and A4).
- S5– Add an Additional Data Channel, NOT Band and Channel Spacing Compliant (building blocks B3, C1a, C1b, C2, C3, C4, C5, and C6).

These solution sets can then be combined into four potential solutions:

- L1 – Optimum Existing Case: this solution combines adding a new message (A2b) from S1 and an increased data rate (B1) of 200 bps from S2 to the existing MSK signal.
- L2 – Narrow Aiding Channel: this solution consists of adding CW signal(s) to the existing MSK signal (B5 from S3).
- L3 – Combination: this solution is a combination of L1 and L2.
- L4 – Wide Aiding Channel: this solution is similar to L2 but ignores the bandwidth constraints and could consist of either C5 or C6 from S5.

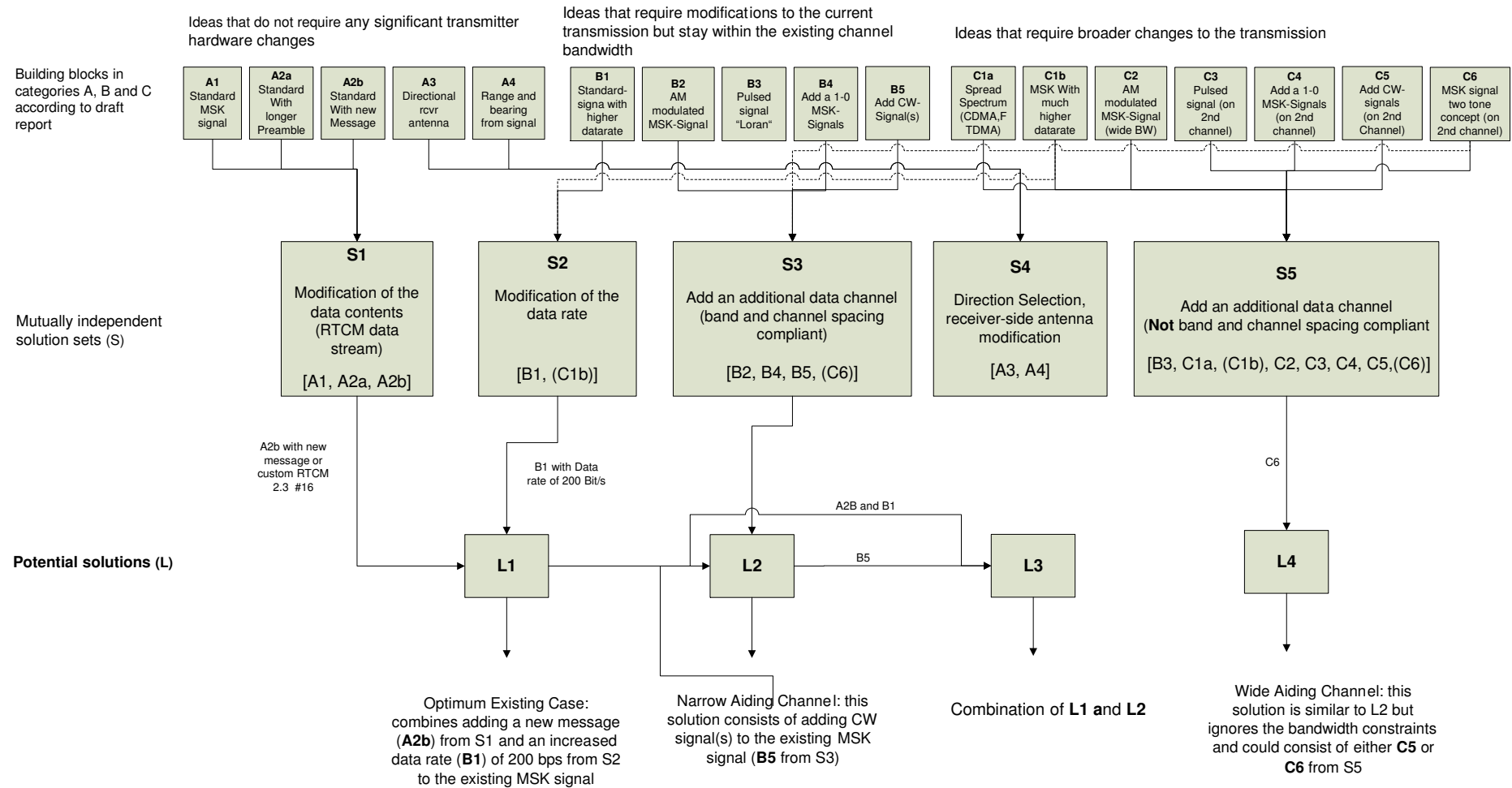


Figure 6: Building blocks mapped to solution sets and proposed solutions.

2.1 Detailed Description of Agreed Upon Alternatives (LP1-310)

2.1.1 L1 – Optimum Existing Case

The DGNSS system transmits its information via a binary modulation method known as MSK; Pasupathy [17] presents a classic overview of this modulation method. At its essence, MSK maps each data bit into a constant amplitude sinusoidal signal of duration T_s seconds ($1/T_s$ is the corresponding bit rate) with the value of the bit determining the frequency of the sinusoid. During the k^{th} bit interval, the signal would be of the form:

$$s(t) = \begin{cases} A \sin(\omega_0 t + \phi) & ; \quad k^{\text{th}} \text{ data bit} = 0 \\ A \sin(\omega_1 t + \phi) & ; \quad k^{\text{th}} \text{ data bit} = 1 \end{cases}$$

In this modulation method the two frequencies, ω_0 and ω_1 , are chosen to be close together (to limit the required bandwidth of the system), yet yield orthogonal signals (to increase the ability of a receiver to discern which signal was transmitted). Further, a phase shift ϕ is included so that the resulting signal has continuous phase from one bit period to another. Letting b_k represent the k^{th} bit in the binary data sequence mapped to positive or negative one ($b_k = \pm 1$), the precise functional form for the MSK signal is:

$$s(t) = A \sin\left(\left(\omega_c + b_k \frac{\pi}{2T_s}\right)(t - kT_s) + \phi_k\right)$$

This expression holds for time in the k^{th} bit interval, $kT_s < t < (k+1)T_s$. The other parameters are amplitude A , center frequency ω_c ($2\pi f_c$ Hz), and the constant $\phi_k \in \left\{0, \pm \frac{\pi}{2}, \pi\right\}$ which represents the accumulated phase due to prior bits needed to maintain the phase continuity.

For its use as a communications link, receivers must be able to demodulate the MSK transmission. While the concept of modulation using two distinct frequencies is simple, the continuous phase nature of the signal makes optimum decoding more complex than that of amplitude modulation; hence, the plethora of decoding methods presented over the past 30 years [18-26]. In typical MSK communications systems the transmitter is not “precisely” controlled by a highly stable timing/frequency source (with respect to precisely controlling the modulation frequency and phase and the times of the bit transitions). As such, typical MSK demodulators are constructed to track the variation of the slowly varying signal characteristics [27]. For the communications application, being “pretty close” in frequency, phase, and bit timing is often good enough; the loss in communications performance due to a mismatch being small [28].

Since about 1990, and in response to an interest in systems able to process bursts of data, there has been considerable effort on developing methods to more precisely estimate the MSK signal’s parameters of time of bit transition, frequency, and phase. Unfortunately, due to the signal’s complexity, there is no known maximum likelihood estimate; instead, computationally efficient, suboptimum estimators have been developed [29-41].

Assuming that the MSK transmission is controlled by a precise timing/frequency source, both the times of the bit transitions (potentially once every T_s seconds) and the underlying phase of the transmitted signal could be exploited to estimate the time of arrival (TOA) for ranging applications. Knowledge of how effectively an estimation algorithm performs can be combined with information on the geometry of the transmitter locations to predict overall positioning performance. Without a broadcast time message, the time of bit transition has an ambiguity of the symbol period, 0.01 seconds (a 3000 km lane), for 100 bps MSK. Given that the propagation range for DGNSS is measured in the 100s of km, the bit transition time is

unambiguous. However, the signal phase does repeat every cycle; at 300 kHz the lane width is 1 km, so the cycle ambiguity must be addressed if using the carrier phase.

The topic of parameter estimation from noisy observations has a long history in the engineering and statistics literature (see e.g. [42]). How much is known about the best algorithm for estimating a particular parameter and how well that algorithm performs depends upon the precise relationship of the parameter to the signal itself and the environment in which the signal is received. A standard requirement when selecting or developing an estimator is that it be unbiased; that the error, on average, equal zero. A common estimation theory approach is to use the maximum likelihood estimate (MLE), the value of the parameter that maximizes the probability of the observed signal. Unfortunately, the MLE cannot be found for all problems and is not always unbiased.

A common measure of performance for an estimator is its second moment (variance); this is certainly relevant for the positioning application as we typically describe positioning accuracy in terms of the 2 drms error. While it may be difficult to develop an exact expression for the variance for a specific estimator, it is often possible to compute a lower bound to it. The Cramér-Rao Bound (CRB) is a lower bound to the variance of any unbiased estimation algorithm. In some instances the CRB is too difficult to compute directly because of the existence of additional unknown parameters (called nuisance parameters, in this case the data bits themselves). A second option that may be computable, the “modified” CRB (MCRB) [43, 44], provides a lower bound to the CRB by averaging over these nuisance parameters.

2.1.1.1 TOA estimation from bit-edge

As described above, a number of authors have presented algorithms to estimate the times of the bit transitions for MSK. As the CRB for this transition time estimate, \hat{t} , is too difficult to compute directly, the MCRB was developed in [43, 44]; the result from [34] is:

$$\text{var}(\hat{t}) = \sigma_{\hat{t}}^2 \geq \text{MCRB}(\hat{t}) = \frac{2}{\pi^2 L_0 T \text{SNR}}$$

in which L_0 is the number of symbol periods observed (i.e. the number of potential bit transitions in the data – the signal model assumes that the data is random), T is the observation period, and SNR is the receiver signal-to-noise ratio. To assess how well the time of the bit transition of a 100 and 200 bps DGNSS broadcast can be estimated, this bound was computed for a 5 second observation period (L_0 of 500 and 1000, respectively). Figure 7 shows the resulting standard deviation (square root of the variance) in seconds versus SNR (in dB). Note that doubling the bit rate while maintaining the observation period reduces the variance by a factor of 2; the standard deviation shrinks by $\sqrt{2}$.

Although increasing the bit rate from 100 to 200 bps reduces the energy per bit (by 3dB, thus slightly reducing performance of the communications channel, possibly resulting in reduced coverage range), the total energy in the signal remains the same and does not impact the ranging performance.

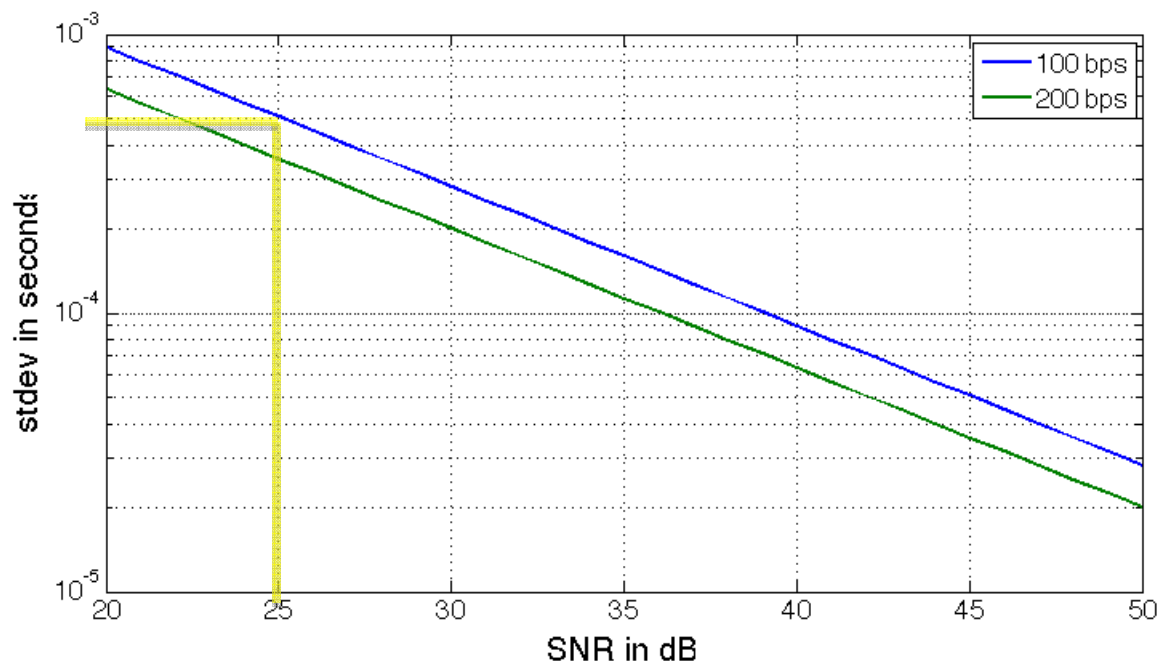


Figure 7: The modified CRB for estimating the time of a bit transition. At a typical SNR of 25 dB, the standard deviation would be 0.5 msec, which equates to about 150 km.

Depending upon the received SNR, the MCRB for the 100 bps DGNSS signal yields standard deviations in the 10's to 100's of microseconds range. This is too large for a positioning application, but still fine for communications systems as this is only a small percentage of the 10 msec bit interval; increasing the bit rate to 200 bps only improves the bound by a small factor. Further, recall that these MCRB values are not particularly achievable. For example, Figure 8 (a reprint of Figure 5 from [34]) compares the estimation variance versus the bit energy to noise ratio (a different scale than that of Figure 7), showing both the MCRB (the solid line) and results from simulations of the time of bit transition estimation algorithm described therein (the circles and squares). Of significance in this figure is the loss of performance from the MCRB to actual of approximately 3-5 dB.

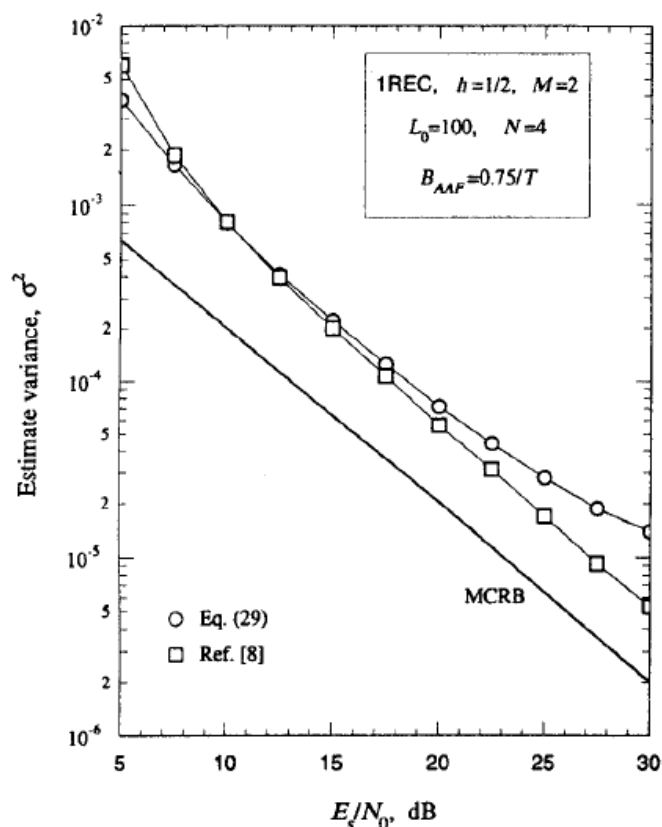


Figure 8: A comparison of the MCRB and achievable performance (reprint of Figure 5 from [34]).

2.1.1.2 TOA estimation from carrier phase

As a second option, one could consider estimating the sinusoidal signal's phase angle, resolving the cycle ambiguity some other way. To be able to effectively estimate the phase requires the assumption of data-aiding; that the MSK data be known accurately at the receiver via demodulation so that individual bit periods can be identified as corresponding to either data "0" or data "1" for further processing. In that way, all observations of the signal during "0" periods (sinusoids at frequency ω_0) can be combined for processing; the same holds for all periods with data equal to "1" (and frequency ω_1).² Fortunately, under the assumption of perfect data demodulation, this data sequence is known and can be accounted for. Further, since the times of the bit transitions are not known perfectly (see the discussion above) some portion of each bit period must be ignored, acting as a guard band or interval, to ensure that phase estimation processing only combines data with the same frequency sinusoid. At best the entire data record consists of usable data for phase estimation; more realistically, there may be a loss of a few percent (it was noted above that the ability to accurately estimate the time of a bit transition is good to within a few percent). The question to be considered here is the possibilities of using this phase information.

² Strictly, depending upon the actual data sequence, non-adjacent bit periods at either frequency will exhibit phase jumps, equal to integer multiples of 90° , which needs correcting before data processing.

Once again, the complexity of the MSK signal itself precludes a direct CRB to the ability to estimate the underlying signal phase, $\hat{\phi}$; however, a MCRB (measured in radians) is available [43, 44]:

$$\text{var}(\hat{\phi}) = \sigma_{\hat{\phi}}^2 \geq \text{MCRB}(\hat{\phi}) = \frac{1}{2L_0T_s\text{SNR}}$$

where, in this case, $L_0T_s = T$ is the total observation period. Converting this MCRB from angle (in radians) into time depends upon the frequency (ω_c , measured in radians per second) of the sinusoid:

$$\sigma_{\hat{\tau}}^2 \geq \frac{1}{2\omega_c^2 T \text{SNR}}$$

Assuming a nominal DGNSS frequency of 300 kHz yields the curve shown in Figure 9 (again for a measurement period of 5 seconds). When compared to Figure 7, this result appears to be about 5 orders of magnitude better from a positioning perspective; with the standard deviation in the nanoseconds range. Of course, one must recall that the phase yields an ambiguous pseudorange, potentially off by integer multiples of the wavelength of the signal. At 300 kHz, this wavelength is 1 km.

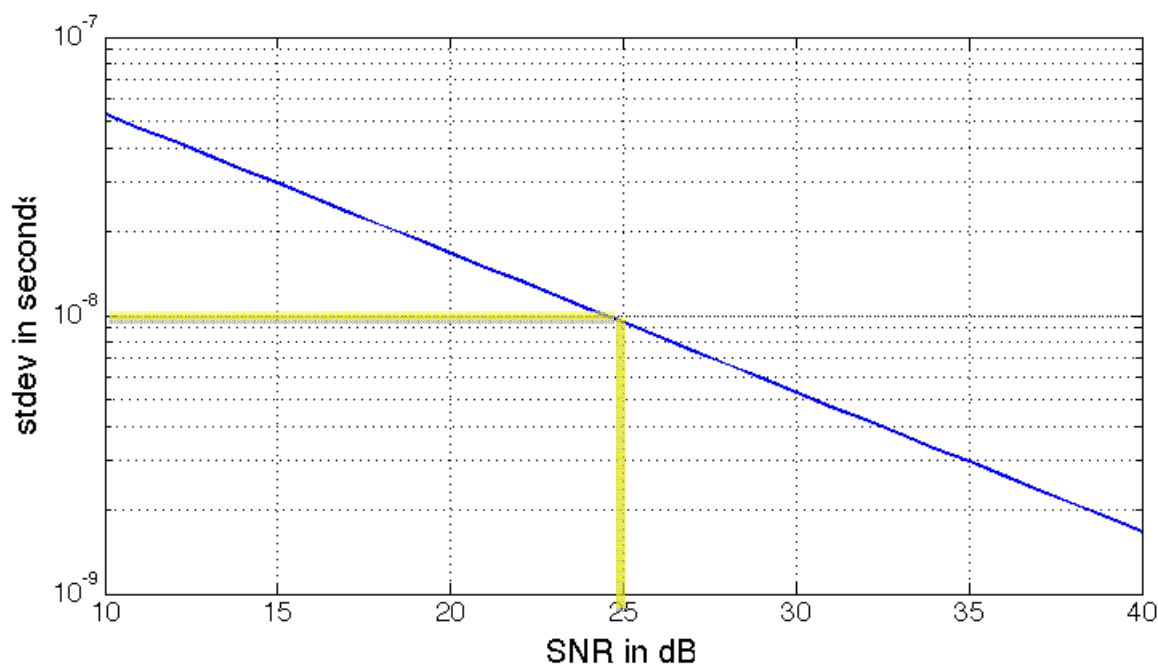


Figure 9: The modified CRB for estimating the time from the phase. For the same typical 25 dB SNR, the standard deviation is ~9 nanoseconds which equates to ~2.7 meters.

Again, recall as above that these MCRB values are not particularly achievable. While no direct result was found in the archival literature comparing achievable estimates to the bound (as was shown in Figure 8 for time of bit transition estimation), one would expect that the performance would be somewhat higher than the “lower” bound.

Recognizing the limited resolution available with estimates of the times of the bit transitions, and the multiple periods of the sinusoid within a bit period (e.g. approximately 3000 cycles

per bit for 100 bps MSK at 300 kHz), the issue of cycle ambiguity of the phase estimate is a severe one. In the Omega system [45] this was addressed in several ways:

- Initializing the receiver at a fixed location and “counting” cycles as the platform moved.
- Using time synchronized, multiple frequency signals and solving for a position that simultaneously satisfied all of the ambiguity equations with integer solutions. This was accomplished in the Omega system by using different frequencies from spatially separated transmitters.

2.1.1.3 New Message on Existing MSK

One approach with MSK would be to employ the bit transition times to fix the cycle and use the phase estimate as the precise time. However, timing errors from the bit transitions measured in the 1000s of nanoseconds will be insufficient for resolving this ambiguity. Better bit timing is needed.

An alternative for pseudorange estimation from standard DGNSS broadcasts is to employ a deterministic DGNSS message (all bits known). To discuss this in the context of the ranging application, let us employ the notation:

$$r(t) = s(t - \tau) + n(t)$$

in which $r(t)$ is the received signal, $s(t)$ is the known signal, τ is the random time delay parameter that we wish to estimate, $n(t)$ is noise, and the observation period is $0 < t < T$.

To begin the discussion we review results on MLEs of time of arrival for deterministic signals from Whalen [46]. First, assuming that $n(t)$ is a white Gaussian noise random process, the MLE for τ , $\hat{\tau}$, must satisfy the equation

$$\int_0^T r(t) \frac{\partial s(t - \hat{\tau})}{\partial \tau} dt = 0$$

Further, the CRB on the variance of the estimate can be written as

$$\sigma_{\hat{\tau}}^2 \geq \left\{ \frac{2}{N_0} \int_0^T \left[\frac{\partial s(t)}{\partial t} \right]^2 dt \right\}^{-1}$$

Now, consider a deterministic MSK message. Recalling the form of the signal with a known data sequence, $b_k = \pm 1$ for integers $k = 0, 1, \dots, N - 1$:

$$s(t) = A \sin \left(\left(\omega_c + b_k \frac{\pi}{2T_s} \right) (t - kT_s) + \varphi_k \right)$$

the necessary condition for the MLE can be expressed as:

$$\begin{aligned} & \sum_{k=0}^{N-1} \omega_k \cos \omega_k \tau \int_{kT_s}^{(k+1)T_s} r(t) \cos(\omega_k(t - kT_s) + \varphi_k) dt \\ & = \sum_{k=0}^{N-1} \omega_k \sin \omega_k \tau \int_{kT_s}^{(k+1)T_s} r(t) \sin(\omega_k(t - kT_s) + \varphi_k) dt \end{aligned}$$

in which we have defined the actual frequency in the k^{th} bit slot as

$$\omega_k = \omega_c + b_k \frac{\pi}{2T_s}$$

Comparing this to the CW result above, we see similar sine and cosine correlations on each bit interval, but with the added complication of a weighted sum over the bit intervals. The CRB can be computed to be:

$$\sigma_{\hat{\tau}}^2 \geq \left\{ \frac{2}{N_0} \sum_{k=0}^{N-1} \frac{A^2 T_s}{2} \left(\omega_c + b_k \frac{\pi}{T_s} \right)^2 \right\}^{-1}$$

Since the only dependence of this expression upon k is through the b_k , we can count terms. Let N_+ and N_- represent the number of times $b_k = +1$ and $b_k = -1$, respectively ($N_+ + N_- = N$). Then

$$\int_0^T \left[\frac{\partial s(t)}{\partial t} \right]^2 dt = N_+ \frac{A^2 T_s}{2} \left(\omega_c + \frac{\pi}{T_s} \right)^2 + N_- \frac{A^2 T_s}{2} \left(\omega_c - \frac{\pi}{T_s} \right)^2$$

We can bound this result for any message sequence as

$$N \frac{A^2 T_s}{2} \left(\omega_c - \frac{\pi}{T_s} \right)^2 \leq \int_0^T \left[\frac{\partial s(t)}{\partial t} \right]^2 dt \leq N \frac{A^2 T_s}{2} \left(\omega_c + \frac{\pi}{T_s} \right)^2$$

Further, since $\omega_c \gg \frac{\pi}{T_s}$ for our problem of interest

$$\int_0^T \left[\frac{\partial s(t)}{\partial t} \right]^2 dt \approx N \frac{A^2 T_s}{2} \omega_c^2 = \frac{A^2 T}{2} \omega_c^2$$

so

$$\sigma_{\hat{\tau}}^2 \geq \frac{1}{2\omega_c^2 T SNR}$$

As expected, we get better estimates (smaller $\sigma_{\hat{\tau}}^2$) if we have higher SNR, higher frequency (ω_m), and/or longer observation time (T). Further, this expression is equivalent to the MCRB for the phase of the MSK signal above in Figure 9. As an example, for a typical receiver with 5 second averaging and 25dB SNR, the bound equates to pseudorange of ~9 nanosecond (3 meters) accuracy.

L1 – Optimal Existing

Performance bounded by: $\sigma_{\hat{\tau}}^2 \geq \frac{1}{2\omega_c^2 T SNR}$

Using either phase or bit-transition (known message) estimates

Cycle resolution on phase using bit-transition estimate

2.1.2 L2 – Narrow Aiding Channel

An alternative approach to improve ranging is to add CW transmissions into the MSK band, estimating the time delay from the phase and separately resolving the ambiguity. Ideally the CW signals would be added at frequencies that fall in the nulls of the MSK spectrum so as to reduce their impact on legacy DGNSS users. As an example, Figure 10 shows the spectrum for an MSK signal (at 200 bps) with two added sinusoids at offsets of -250 and $+250$ Hz from the center frequency, respectively. In order to do lane resolution effectively, these frequencies should be spaced as far apart as possible; ± 250 Hz is the maximum spacing that is still within the 500 Hz band. These CW frequencies fall in the nulls of a 200 bps MSK signal.

A second, adjacent channel of MSK (at 100 bps) is shown in green in Figure 10. If the adjacent channel signal is not at the same bit rate, then the nulls do not align (as shown) and the CW falls on part of the adjacent channel's signal. Fortunately, the adjacent channel is too low in power to impact the CW ranging signal, and the CW ranging signal is too far from the center of the adjacent channel to adversely impact the adjacent channel. If the adjacent channel signal was at the same bit rate (not shown), then the two MSK signals would have overlapping nulls and the CW signals would neither impact, nor be impacted by, the MSK signals.

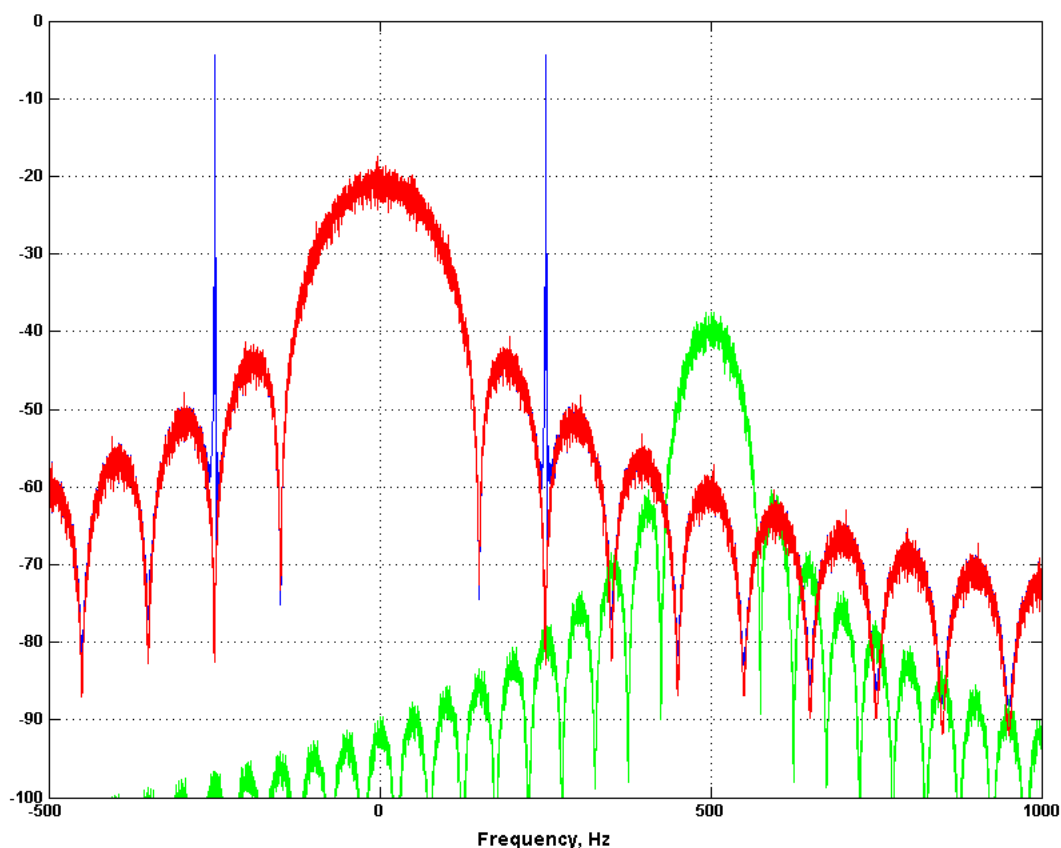


Figure 10: MSK Spectrum in red, CW Signals in blue, adjacent channel MSK with its own CW in green.

To analyse this approach, consider a single CW signal consisting of k complete cycles of a sinusoid of known frequency ω_m :

$$s(t) = A \sin(\omega_m t) \text{ for } 0 < t < \frac{2\pi k}{\omega_m} = T .$$

For this signal, the MLE of the time delay must satisfy the condition:

$$\int_0^T r(t) \frac{\partial s(t - \hat{\tau})}{\partial \tau} dt = -A\omega_0 \int_0^T r(t) \cos \omega_m(t - \hat{\tau}) dt = 0$$

This result can be expressed as [47]:

$$\hat{\tau} = -\frac{1}{\omega_m} \tan^{-1} \left(\frac{\int_0^T r(t) \cos \omega_m t dt}{\int_0^T r(t) \sin \omega_m t dt} \right)$$

The CRB for this problem can be computed to be:

$$\sigma_{\hat{\tau}}^2 \geq \left\{ \frac{2}{N_0} A^2 \omega_m^2 \frac{T}{2} \right\}^{-1} = \frac{N_0}{2A^2 \omega_m^2 T} = \frac{1}{2\omega_m^2 T SNR}$$

which is identical to the MCRB for the time estimate from the phase of the random MSK signal above (except for a constant) and to the CRB of the time delay estimate for the fixed DGNSS message. The obvious advantage of working with a CW signal over the MSK phase estimate is the simplicity of the estimator. The disadvantage with respect to the deterministic MSK message is the ambiguity of the sinusoidal phase; at 300 kHz, this ambiguity is multiples of 1 km.

One approach to resolving ambiguity is to generate multiple, synchronous sinusoids at each transmitter and to examine the beat frequency³ of those signals at the receiver. If two CW transmissions are 500 Hz apart (as suggested in Figure 10), then the lane width for the beat signal is 600 km. Estimating the phase of this beat frequency to a fraction of a degree would provide a unique lane for the 300 kHz signal. The bit synchronization would identify the correct 600 km lane, see Table 2.

L2 – Narrow Aiding Channel Case

Performance bounded by: $\sigma_{\hat{\tau}}^2 \geq \frac{1}{2\omega_c^2 T SNR}$

Using phase estimates on CW, which is easier to implement than phase estimate on MSK carrier

Cycle resolution using beat frequency (product) of two CW signals

³ If two signals are multiplied together, the result is a signal consisting of sinusoids of the sum and difference of the two original frequencies, which can be separated by filtering and used as two new individual frequencies.

Table 2: Accuracy and Lane Resolution.

Method	Freq.	Wave length = lane width (km)	Accuracy - % of period	Accuracy (ns)	Accuracy (m)	Notes
Bit synch	100	3000.0	0.14%	13888.89	4166.7	If bits are UTC synched then this gets us to nearest 4km – not enough to resolve lane of single frequency but is enough to resolve lane of difference beat frequency
Carrier (fc)	300 kHz	1.0	0.14%	4.63	1.4	Single frequency gives sub 2m accuracy, but 1km lane width
CW1	fc + 250 Hz	1.0	0.14%	4.63	1.4	Single frequency gives sub 2m accuracy, but 1km lane width
CW2	Fc - 250 Hz	1.0	0.14%	4.63	1.4	Single frequency gives sub 2m accuracy, but 1km lane width
CW1+ CW2	600 kHz	0.5	0.14%	2.31	0.7	Beat frequency (product) gives sub-meter accuracy, but 500m lane width
CW1- CW2	500 Hz	600.0	0.14%	2777.78	833.3	Beat frequency (difference) has resolution to get into the correct lane for the single frequency

2.1.3 L3 – Combination

This solution is a combination of L1 and L2, employing both the new RTCM message and one additional CW signal:

- As noted in 2.1.1.3, estimating the time delay from the new RTCM message could provide a high accuracy pseudorange measurement; the disadvantage of such is the need to frequently transmit this new message, which reduces the data throughput of the DGNSS channel.
- As noted in 2.1.2, it is quite a bit easier to estimate the phase of a CW transmission rather than having to take into account the data-driven frequency changes in the MSK transmission; the disadvantage of a single CW transmission is the need to resolve the lane ambiguity, approximately 1 km for signals in the DGNSS band.

The L3 approach uses the advantages of each of these to resolve the other's disadvantage. Specifically, the approach is to do a fine pseudorange estimate from the phase of the CW signal (converted to distance) and resolve the ambiguity from occasional measurements of pseudorange from the new MSK signal. Unless the vehicle has extremely high dynamics, its change in position does not result in lane jumps; hence, from estimate to estimate the CW phase changes little and the lane can be tracked. Occasional transmission of the new message would allow for an unambiguous pseudorange calculation that could be used to verify the lane tracking of the CW phase estimate. This occasional transmission has a small effect on DGNSS throughput. Further, since there is only one CW transmission, its frequency can be set within the channels band and at one of the MSK spectral nulls.

L3 – Combination of L1 and L2

$$\text{Performance still bounded by: } \sigma_{\hat{r}}^2 \geq \frac{1}{2\omega_c^2 T SNR}$$

Uses phase estimates on CW, which is easier to implement than phase estimate on MSK carrier

Cycle resolution resolved from bit-transition estimate of new message – this need only be transmitted occasionally

2.1.4 L4 – Wide Aiding Channel

This solution is similar to L2 but ignores the bandwidth constraints and could consist of either C5 or C6 from S5. Allowing additional bandwidth via combining adjacent channels could allow for higher rate MSK transmissions; hence, improving the accuracy of pseudoranges developed from times of bit transitions. Allowing additional, but not adjacent, channel usage could allow for multiple CW transmissions from the same transmitter at different frequencies. If properly spaced in frequency, ambiguity resolution is possible directly from the CW signals. Further, it is feasible that a second MSK channel transmitting the same DGNSS message might provide the same level of performance with a somewhat more complex receiver [7] (the two-tone modulation concept, C6).

2.1.5 Pros/Cons of Solutions

Table 3 contains a summary of the Pro's and Con's of the three solutions.

Table 3: Pro's and Con's of Three Solutions.

Solution	Pro's	Con's
L1	1. Minimal change to existing systems.	1. Difficult to track phase on MSK carrier due to frequency shifts 2. To track bits to same accuracy, need new message – used continuously, so would not be able to use the MSK channel for DGNSS corrections. 3. Need to use new message to do lane (cycle) resolution.
L2	1. CW phase estimate is easier to implement than MSK carrier tracking.	1. Requires addition of 2 CW signals. 2. Lane resolution requires high accuracy on phase estimation. 3. R-Mode not possible on adjacent channels.
L3	1. CW phase estimate is easier to implement than MSK carrier tracking. 2. Only need to use the new message occasionally for cycle resolution, preserving MSK channel for DGNSS corrections. 3. Only single CW signal needed, can use R-Mode on adjacent channels.	1. Requires some change to existing system: addition of 1 CW signal and occasional use new message.

Recommended Solution is L3

Performance bounded by: $\sigma_{\hat{\tau}}^2 \geq \frac{1}{2\omega_c^2 T SNR}$

Use phase estimate on single CW

Cycle resolution using bit transition on new message (periodically not continuously)

2.2 Elaboration of Requirements for Time Synchronization (LP1-320)

In order to do positioning from multiple ranges or to establish time from a single range, the times of transmission must be precisely timed. There are two timing concerns: time stability and time synchronization.

2.2.1 Time stability

Time stability is important to ensure that the signal does not drift appreciably over the receiver averaging time (perhaps 5 seconds). For this purpose, time stability on the order of one nanosecond over the 5-seconds would be more than sufficient. If we can measure

range to 100ns then time accuracy needs to be better than 1ns. This equates to clock stability at the transmitter of $\sim 1 \times 10^{-10}$. This would argue for a Rubidium (Rb) clock (typical performance of 1×10^{-11}) at the transmitter, not a Caesium (Cs) clock (typical performance of 1×10^{-13}). Most DGNSS transmitters currently use Oven Controlled Oscillators (OCXOs), which only have a time stability of 1×10^{-7} so would need to be upgraded to a new DGNSS modulator that either contains a Rb clock or can accept and synchronize to an external Rb which would need to be added to the equipment suite.

2.2.2 Time synchronization

Time synchronization is needed to determine Universal Coordinated Time (UTC) from the received signal and to eliminate relative clock biases between the various transmitters, which otherwise would add to the position error (1 m for every 3.3ns). There are two methods to accomplish this: synchronize each transmitter to a known common time signal such as UTC or use common reference site(s) to sort out the time differences.

2.2.2.1 Synchronize to UTC

In the North Sea Area, the geometry of the stations is good, so for 20m performance we need better than 50ns of accuracy in the clock synchronization to UTC. This could potentially be done using a network time synchronization (using IEEE 1588 PTP) although this is beyond the accuracy of most Precise Time Protocol (PTP) implementations. Two-way Satellite Time Transfer (TWSTT) could be used, but would require point-to-point satellite links between each transmitter and the UTC reference clock. This could also be done using an eLoran time receiver; if the eLoran clock is synchronized to UTC then this would provide a UTC reference, but if not, it would still provide a common reference to all DGNSS transmitters. And finally, GPS could be used to provide the time synchronization up until the point in time that the GPS signal is lost. After this point the signal would remain in tolerance for ~ 28 hours for a high quality Caesium clock or ~ 0.28 hours for a Rubidium clock. Any of these options would require a DGNSS modulator that can synchronize both the carrier phase and the bit period to UTC (using a 1PPS signal perhaps) as well as the time sync receiver (IEEE 1588, eLoran, TWSTT, or GPS).

2.2.2.2 Reference Site

The alternative to synchronizing each transmitter is to have one or more reference sites at known locations that can sort out the relative time differences between the various transmitters. Similar to the way that DGNSS can calculate corrections for GNSS, an R-Mode reference site could track the received R-Mode signals and establish the error in them at the receiver. This error would be primarily the clock offset of the transmitter. This clock offset could then be broadcast on the DGNSS data stream. The disadvantage of this approach is that the mobile receiver would only be able to range off of the R-Mode signals that were also received by the reference site (and thus had corrections for) so this limits the coverage of the system to an area near the reference site.

Time synchronization (to within 50-100ns) to a common reference such as UTC is critical for positioning performance.

Time stability (on the order of 1 ns) is necessary to ensure the transmitter jitter does not impact positioning performance

2.3 Performance Factors (LPI-330)

Analyses of MSK performance appearing in the open literature on communications systems consider only the effects of additive noise. Tables of estimates of additive receiver/channel noise are available from the International Telecommunication Union, Radiocommunication Sector ITU-R [52]. Employing signal power prediction models allows one to take into account loss with distance and geography. While some limited research on how to accommodate multipath (sky wave) in the design of a receiver has appeared (e.g. [48]), none of these explicitly address the resulting performance. Lastly, propagation delays are of no concern to the communications application; hence, there has been no consideration of this impact for MSK signals. They are; however, potentially of concern to ranging. The only serious examination of propagation delays that we are aware of are at Loran frequencies (100 kHz), see for example [49-51].

In its specific use in DGNSS systems, the MSK transmission experiences several channel effects. The following sections provide a description of these various performance limiting factors and analyses them as error sources. For the remainder of this report the analysis has been restricted to the geographic area of the North Sea Area; we have used a bounding box of 50-60° N latitude and from 5°E to 15° W longitude.

2.3.1 Time signal

As discussed above, a stable clock is needed to drive the RF modulator; the stability needed is on the order of 1 nanosecond over the averaging time constant of the receiver. This implies a stability rating on the order of 10^{-9} . This is easily achievable by a Rubidium or Caesium clock, but not by a quartz oscillator. Based upon the cost, it would make sense to use Rb clocks.

2.3.2 Time synchronization

The time synchronization is more problematic. Equipment can be found that will synchronize to within 50-100ns of the UTC reference. Getting less error than this is very difficult (and expensive) and may only be realistically achievable by tracking the transmitter clock offsets and transmitting these offsets as R-Mode clock corrections for each beacon site.

2.3.3 Sky wave

Sky wave is the term used to describe the reception of a time delayed version of the original signal at the receiver; the primary cause for DGNSS transmissions is reflection off of the ionosphere. Ignoring noise, a one-hop sky wave (i.e. only one such delayed version as shown in Figure 11) would result in the received signal:

$$r(t) = s(t) + \alpha s(t - t_d)$$

in which α and t_d represent the attenuation and delay of the sky wave, respectively. Sky wave for MF radio has several characteristics:

- It is most significant at night due to changes in the height of the ionospheric layer [52].
- The sky wave's signal appears later in time than the ground wave signal (on the order of 100's of μ sec later) since the propagation path is longer. Figure 12 shows the typical time delays observed versus distance from the transmitter for a one-hop sky wave (this is simply based upon the difference in the lengths of the two paths in Figure 11). Of significance is the relationship of this delay to the length of an MSK bit period; it is a small portion of the 10 msec bit period of a 100 bps DGNSS transmission.

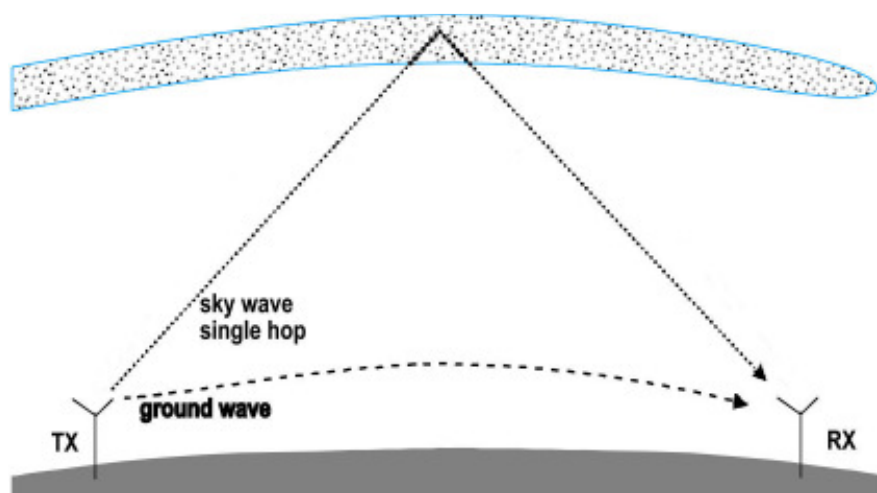


Figure 11: A single hop sky wave.

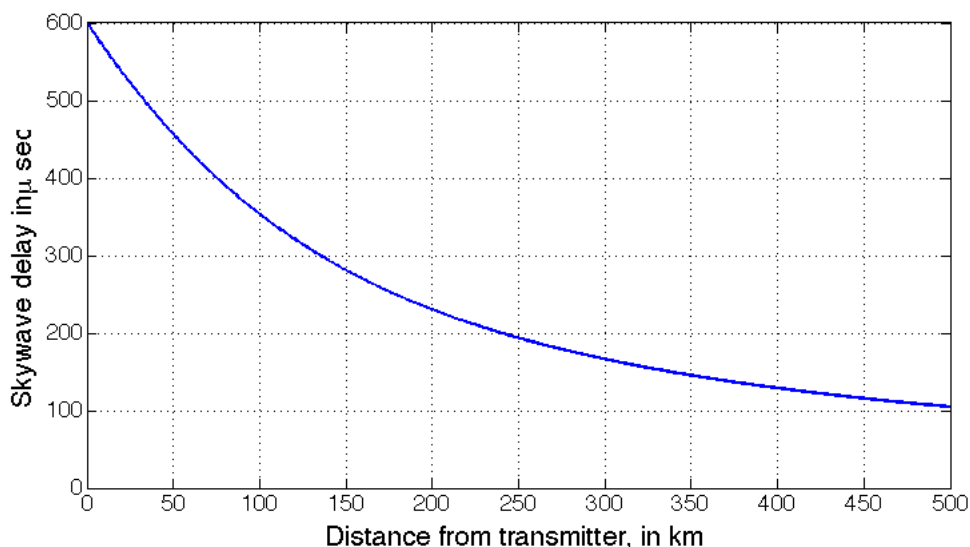


Figure 12: Typical sky wave delay versus distance.

- Its impact is larger at further distances from the transmitter since the ground wave experiences higher attenuation than does the sky wave; the relative signal powers are measured as a fade margin on a dB scale (ground wave minus sky wave power), which can go negative (i.e. the sky wave being stronger than the ground wave). Figure 13 shows possible values of the fade margin versus distance from the transmitter computed using a smooth Earth model and three noise models: FCC, CCIR, and Wang. These were all computed using the LFMF program [53]. We notice that the models provide significantly different results. For the discussion below we will use the worst of these estimates, the CCIR model (this is the same as the model presented in ITU-R P.1147-4 [54]). Further, we employ the actual sky wave's signal strength estimates and combine them with the ground wave's signal strength estimates from 2.3.6 to predict the fading margins as a function of position in the North Sea Area for the predictions of positioning performance in 3.2.

- Since the MSK signal (both random and deterministic message) is continuous in time, the sky wave causes errors in estimates of both the time of bit transition and signal phase; specifically, the late signal crosses the time of bit transition of the ground wave impacting algorithms trying to estimate that time and, within a bit interval, the identical frequency sinusoid can add constructively or destructively (similar statements hold for a CW transmission). Quantification of this effect has not appeared in the literature, nor does it seem easy to accomplish.

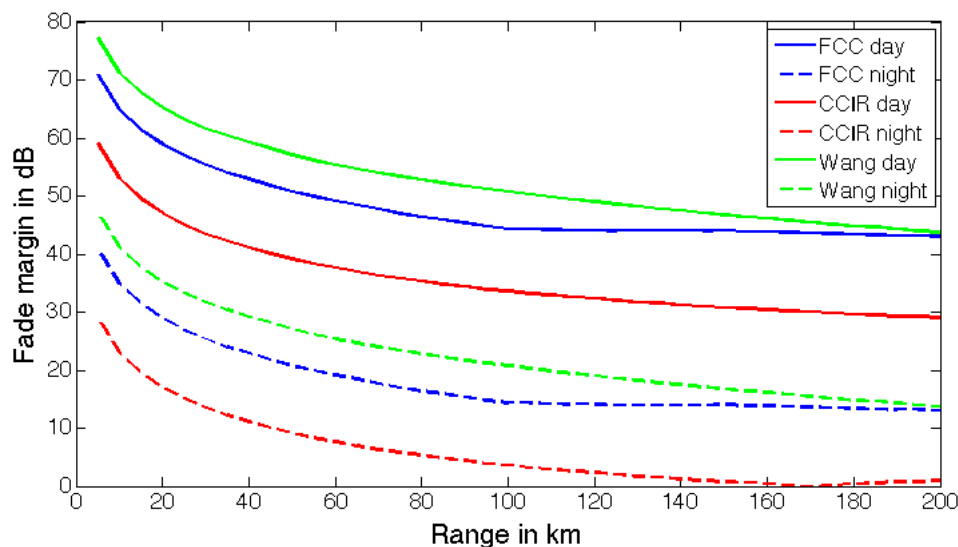


Figure 13: Typical fade margin assuming smooth earth model.

To better understand the impact of sky wave on phase estimation, consider a pair of adjacent bit intervals with different frequencies as shown in Figure 14. In this figure the leftmost vertical solid gray line shows the time of a bit transition; the top trace in the diagram shows the ground wave consisting of two different frequency sinusoids, green and red, respectively. The second trace is the sky wave signal, an attenuated and delayed version of the ground wave; the rightmost vertical gray line marks the bit transition in the sky wave. The third trace is the arithmetic sum of the ground wave and sky wave. Note that during the time between the ground wave's and sky wave's bit transitions, both frequencies are present. The sky wave component causes an amplitude change (apparent in the figure) and a phase shift from the ground wave signal.

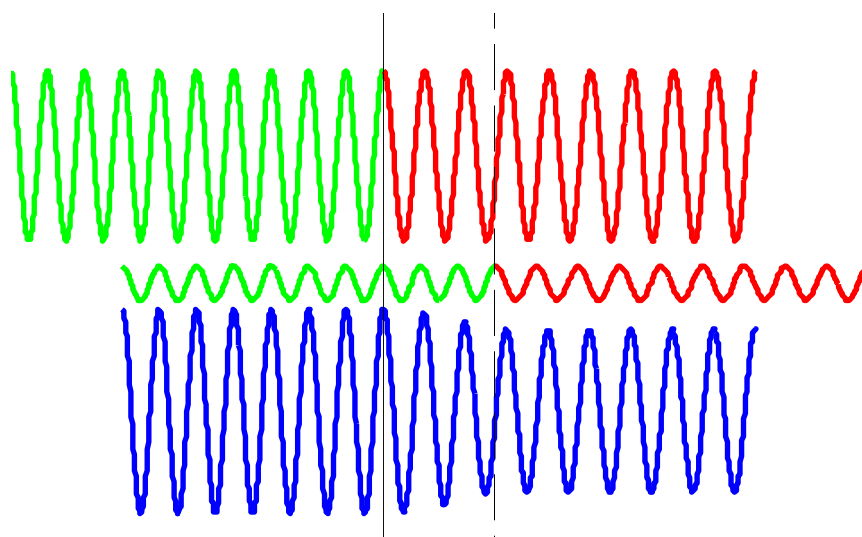


Figure 14: Example of sky wave interference on MSK.

It is possible to be more specific on this effect, see [6]. Ignoring the noise for the moment, and concentrating on one bit interval (a single frequency sinusoid), the received signal is:

$$\begin{aligned}
 r(t) &= s(t) + \alpha s(t - t_d) \\
 &= A \sin(\omega_k t + \phi) + \alpha A \sin(\omega_k(t - t_d) + \phi) \\
 &= \eta A \sin(\omega_k t + \phi + \beta)
 \end{aligned}$$

in which the final line is the result of some trigonometric manipulations; the additional amplitude and phase terms are:

$$\eta = \sqrt{1 + \alpha^2 - 2\alpha \cos(\omega_k t_d)} \quad \text{and} \quad \beta = \tan^{-1} \left(\frac{\alpha \sin(\omega_k t_d)}{1 - \alpha \cos(\omega_k t_d)} \right)$$

In words, within a bit period (i.e. ignoring the overlap of adjacent bit periods for a moment), sky wave contamination results in the received signal being a single sinusoid of the same frequency, but with amplitude scaling η (obvious in Figure 14) and a phase shift of β (less obvious in that figure). If α is small, then the amplitude scaling is nearly unity (and not of too much interest); the impact is constructive or destructive depending upon whether the phase of the interferer is either aligned or opposite to that of the ground wave signal. This 0° or 180° alignment has the most impact on amplitude. In contrast, the phase shift can vary greatly with t_d . This phase variation is periodic in t_d , with misalignment of the two sinusoids (i.e. approximately 90°) causing the largest impact on received signal phase.

It is also possible to develop an expression for the worst-case phase error as a function of the fade margin $1/\alpha$. Figure 15 shows this maximum phase error in nanoseconds as a function of the fade margin and a nominal 300 kHz carrier. Clearly, a minimum fade margin of 15 dB or more is necessary to limit the impact of sky wave on pseudorange estimation to 100 nsec or less. During the day, sky wave effects appear to be sufficiently small so as to not affect performance; however, at night the positioning performance will be negatively impacted.

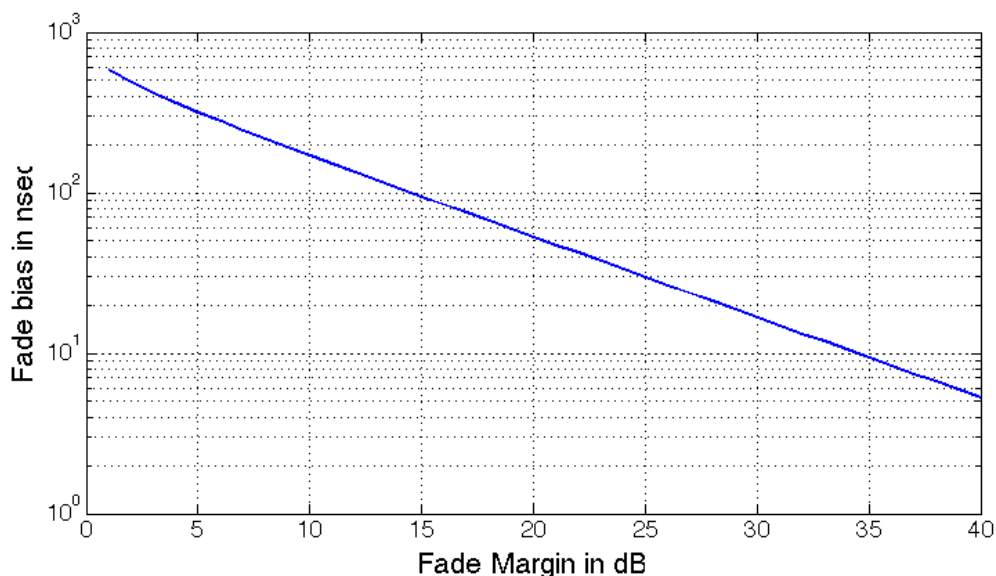


Figure 15: Worst-case time bias as a function of the fade margin.

Sky wave can have a large impact on ranging performance at night

2.3.4 Propagation conditions

The typical method to predict loss of signal power with distance is to use software tools based on Millington's method. These predict loss by using data on ground conductivity along the assumed great circle propagation path.

The speed of propagation of the ground wave is used when converting the time of arrival (TOA) measurements to pseudoranges in the position solution; typically the speed of light is used. This standard value is adjusted for propagation through air by dividing by the index of refraction (this was called the Primary Factor in Loran). In the Loran system, a Secondary Factor was also used, to adjust the speed for propagation over seawater. It is also well known that the non-uniform nature of ground conductivity and topography along the ground wave signal path retards the TOA of transmitted LF and MF signals; this effect is commonly called the Additional Secondary Factor (ASF). There have been numerous studies and reports on these effects for signals at 100 kHz (Loran), most recently in the 2000's with the emergence of eLoran (see, e.g., [50]). Some of these efforts have attempted to numerically compute the ASFs using high resolution ground conductivity and topographical data; unfortunately, the results are not uniformly accurate for the desired positioning performance. Current methods for eLoran create the ASF maps by means of an experimental survey and track/broadcast the temporal variations by means of monitor sites [55]. While this is conceivably an onerous task if the area of interest is large, the combination of established shipping lanes and high correlation of the effects over salt water make this manageable for water environments such as the North Sea. To date we know of no effort to map ASFs for signals near 300 kHz. However, we do expect that the lessons learned from creating ASF maps at 100 kHz will translate directly to 300 kHz.

2.3.5 Interference in 300 kHz band

The primary source of interference in the 300 kHz band is the other DGNSS sites using the same frequency. Since there are 119 active DGNSS beacons and only 65 channels within the frequency band in Region I, there is channel re-use. Figure 16 shows that some of the channels (frequencies) are used by as many as 4 beacons, although most frequencies are used only once or twice (there are also 5 frequencies that are not currently used at all). This co-channel interference is minimized by geographic separation of the sites using the same frequency and conservative transmitter power levels. The largest impact from the co-channel interference tends to be at night when sky waves can increase the signal reception (and thus interference) range. The second main source of interference in Europe is the presence of aeronautical beacons in the maritime band. These impact primarily inland sites and are less of a problem on the coast.

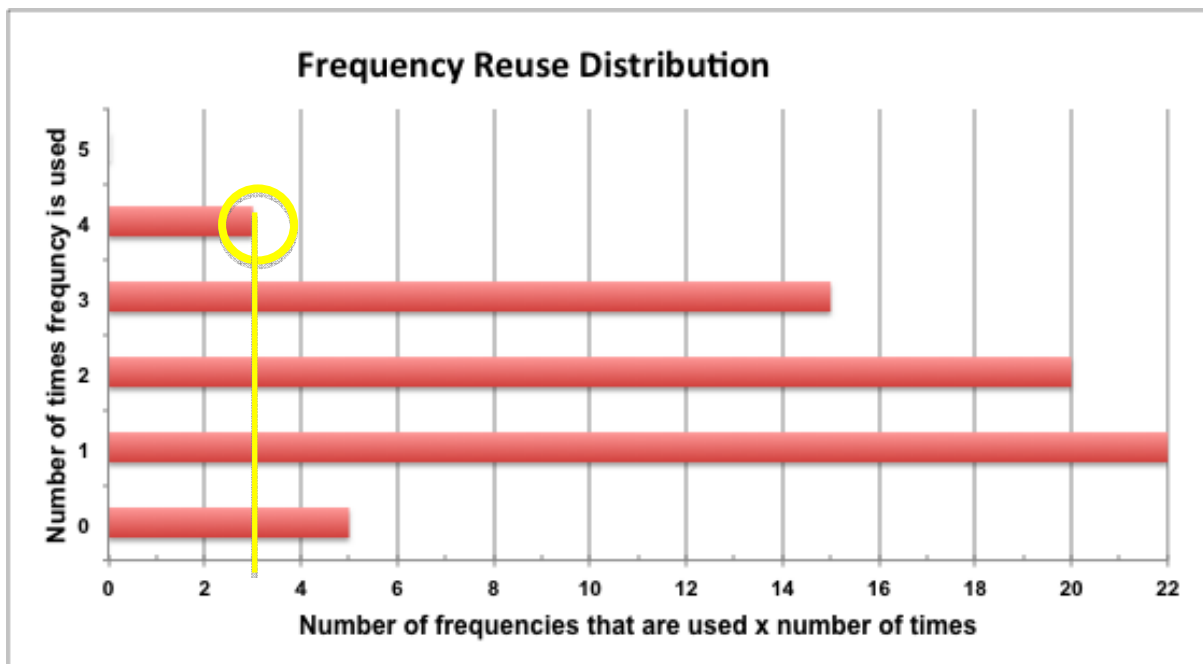


Figure 16: Frequency Reuse Distribution, compiled from IALA listings of DGNSS transmitters. The top bar, for example, indicates that there are 3 frequencies (channels) that are used 4 times each.

2.3.6 Geometry

For a position solution, a large impact on the quality of the solution is the location and relative bearings of the beacon sites to the receiver. This error is captured in the Horizontal Dilution of Precision (HDOP), which is calculated based on the bearings to each of the transmitters. For the North Sea Area, the HDOP has been calculated on a 0.1° by 0.1° grid using only those transmitters providing a signal to noise ratio (SNR) at that location of greater than 7 dB; see Figure 17. Since the HDOP can be interpreted as a multiplier on the user range error, lower numbers are better. As can be seen, most of the coverage area has a very good HDOP (<2). The area of high HDOP off the coast of Denmark could be improved with the addition of a DGNSS beacon in the middle of the North Sea (located in one of the windmill farms perhaps).

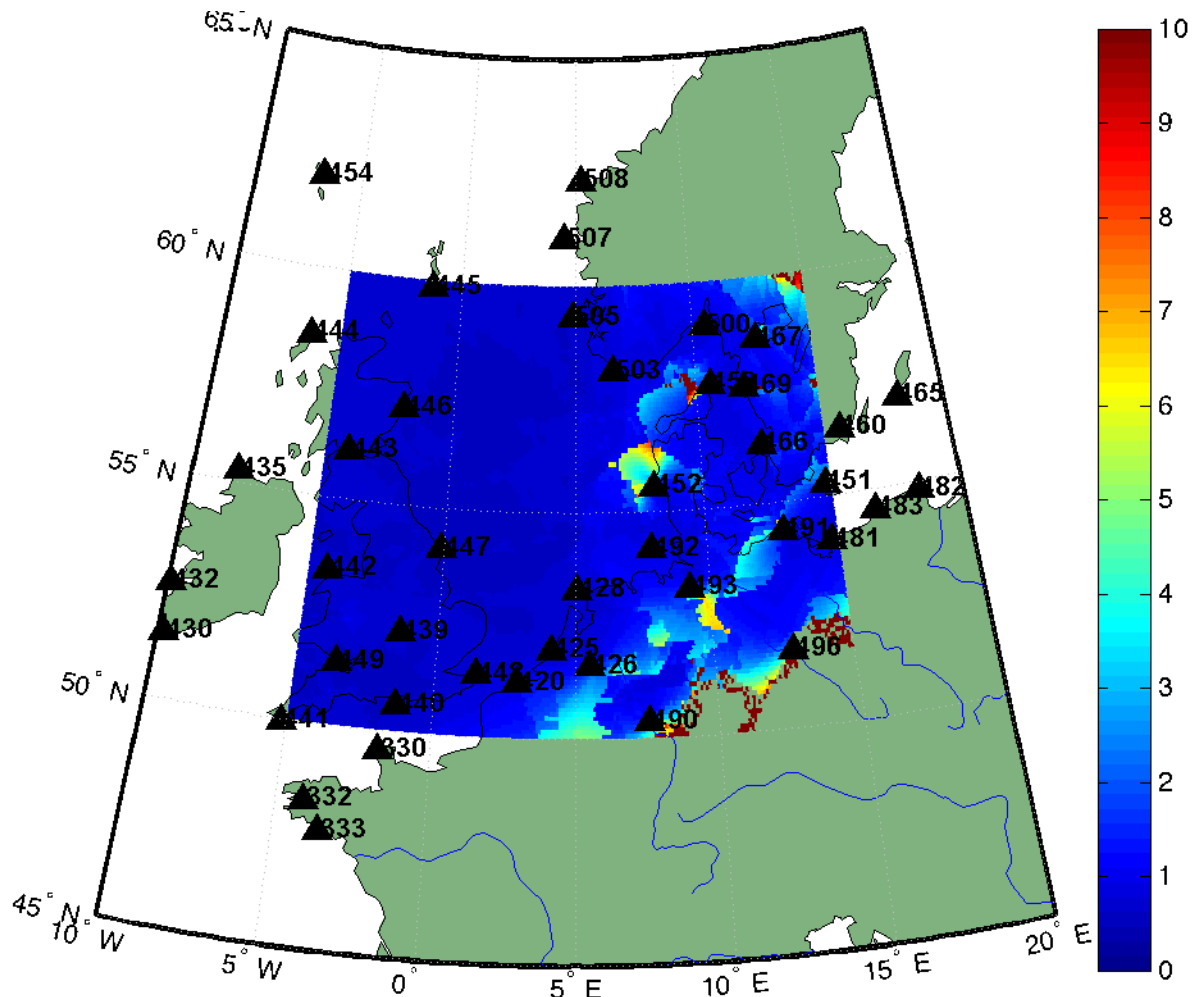


Figure 17: HDOP for the North Sea.

The predicted signal strengths for each beacon were calculated using a MATLAB™ program developed by the authors based on Millington's method [56]; the EIRP for each beacon was estimated based on the stated nominal ranges from the IALA tables of DGNSS Stations⁴. Sample signal strength plots from this prediction program are shown for three beacons in Figure 18.

HDOP values across the North Sea area are quite good (<2).

⁴ Available from <http://www.iala-aism.org/publications/category.html?category=a369e478240722d460335fea600cb81a>

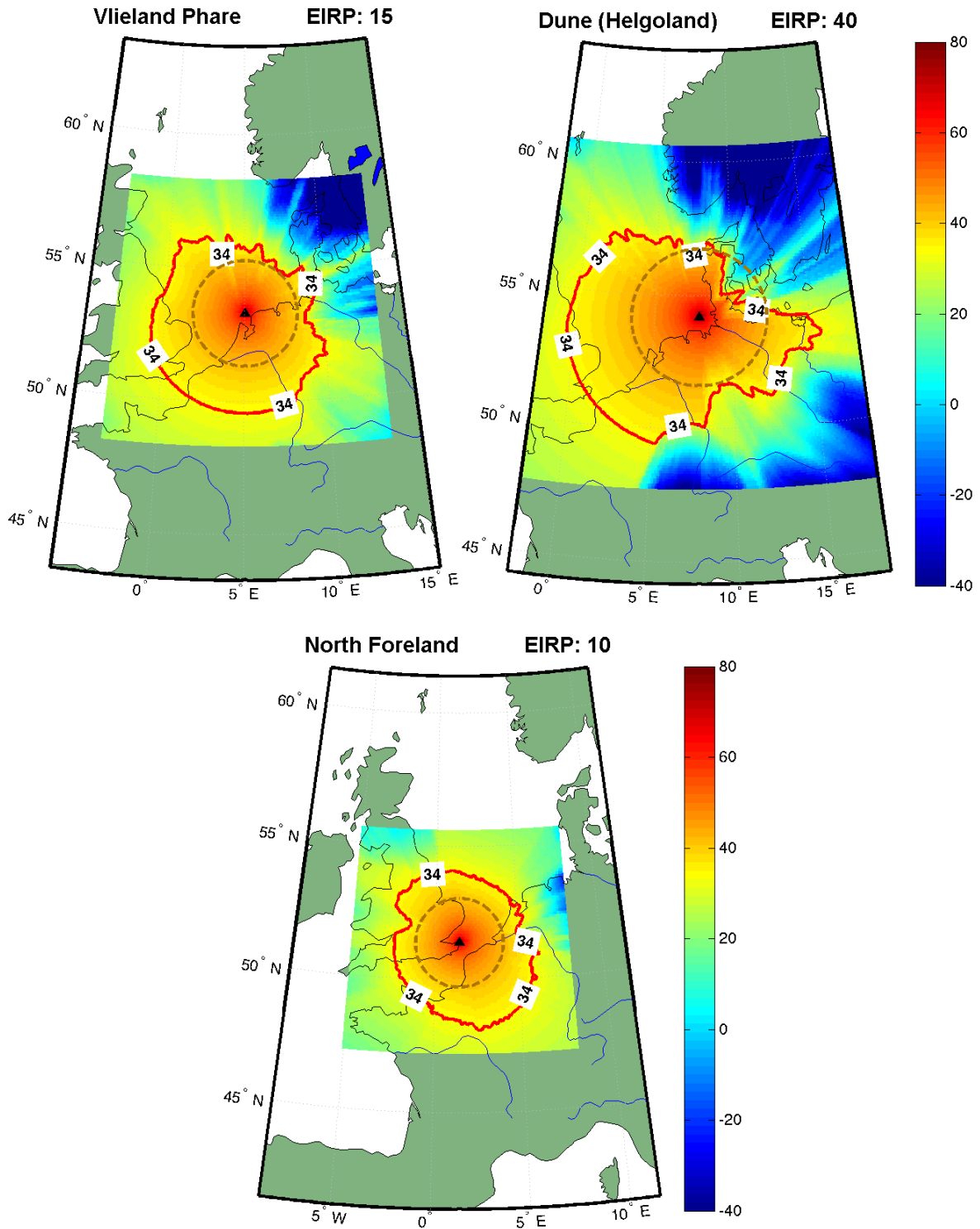


Figure 18: Predicted signal strengths (in dBµV) for three beacons around the North Sea.

The primary input to the Millington's method is the ground conductivity; Figure 19 shows the ground conductivity map that was provided and used for the calculations (with some edits to improve coastline matching)[57]. In this map the numbers correspond to one of the ITU-R conductivity levels as listed in M.832-2 [58]. These are shown in Table 4 with ground type descriptions from [59].

Table 4: Conductivity Map Levels and Descriptions.

Level	Standard values (mS/m)	Lower limit (mS/M)	Upper limit (mS/m)	Ground Type
0				Not defined – treated as sea water
1	5000	3000	7000	Sea water
2	30	17	55	Very good ground
3	10	5.5	17	Wet ground, good dry soil
4	3	1.7	5.5	Fresh water, cultivated ground
5	1	0.55	1.7	Medium dry, average ground, mountainous areas
6	0.3	0.17	0.55	Dry ground, permafrost, snow covered mountains
7	0.1	.055	0.17	Extremely poor, very dry ground
8	0.03	0.017	0.055	
9	0.01	0.0055	0.017	Glacial ice

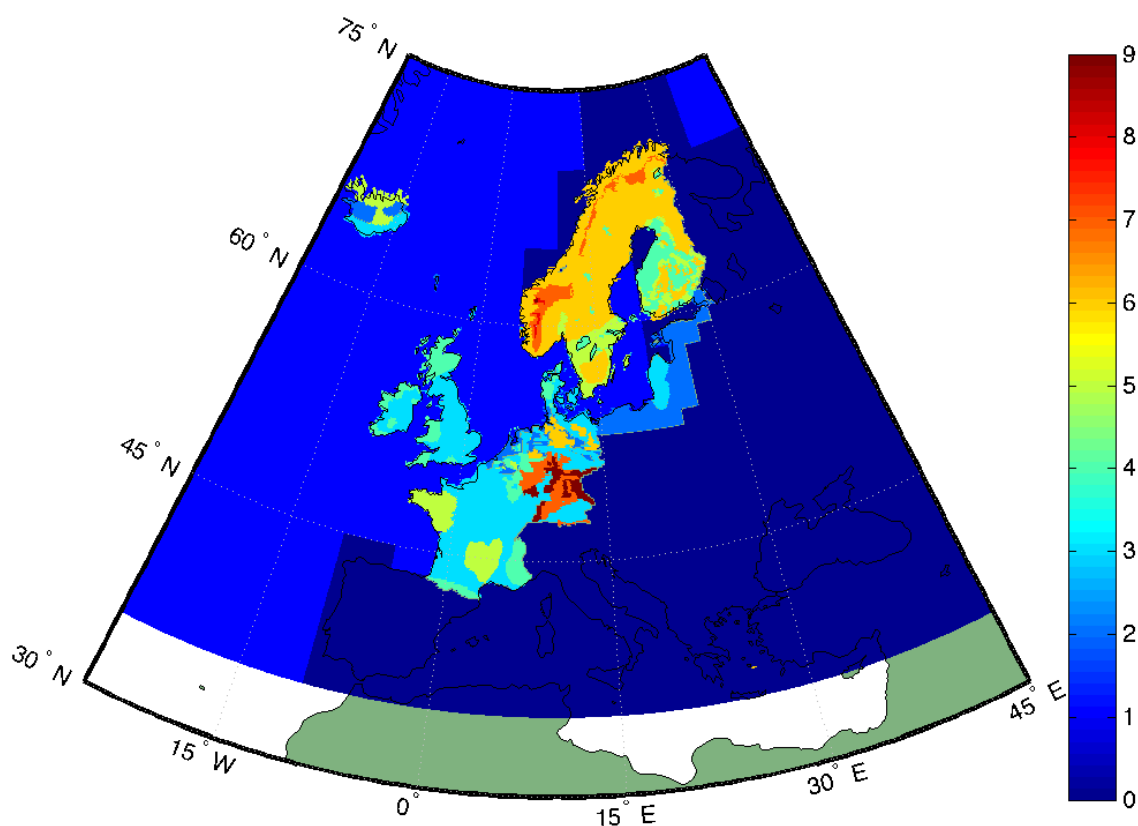


Figure 19: Ground conductivity map; each level maps to one of the ITU-R ground conductivity ranges [58].

The SNR is calculated by subtracting the noise (in dB) from the predicted signal strengths. The noise values used (see Table 5) are from Alan Grant's thesis [59] and are a compilation of the 24 noise maps presented in ITU-R P.372-8 for each season and time period [60]. These noise values are interpolated across the North Sea Area (see Figure 20) and subtracted from the signal strength at each point to get the SNR. An additional uniform noise level of 12dB was added to the location-based value to reduce the SNR to more conservative ranges.

Table 5: Annual average noise values not exceeded 95% of the time, in dB μ V/m, reprinted from [59].

		Longitude (deg)													
		50 W	40 W	30 W	20 W	10 W	0	10 E	20 E	30 E	40 E	50 E	60 E	70 E	80 E
Longitude (deg)	80 N	-3	-2	-4	-4	-4	-4	-3	-3	-2	-3	-3	-4	-6	-7
	70 N	-2	-3	-4	-4	-3	-1	2	4	5	5	4	2	-1	-4
	60 N	-1	-1	-1	1	3	5	9	11	11	10	8	7	2	-1
	50 N	3	3	3	5	7	10	13	13	11	10	9	8	7	4
	40 N	6	6	6	8	11	13	13	13	11	10	9	9	11	13
	30 N	12	11	11	12	13	14	14	13	11	11	11	13	20	24
	20 N	18	14	13	14	17	19	20	19	17	15	17	20	27	30

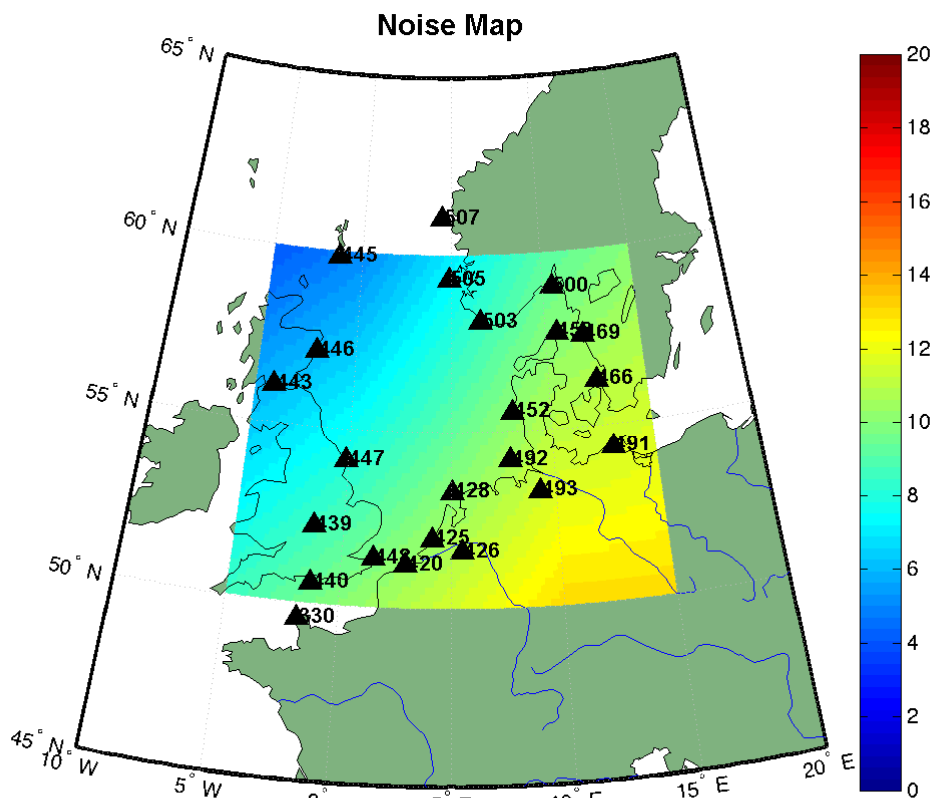


Figure 20: Interpolated noise map, dB μ V/m.

3 Accuracy Analysis (LP1-520)

3.1 Timing Accuracy (LP1-340)

Based on the analysis contained in Section 2, the achievable accuracy on any of the three solutions (L1 – L3) is bounded by the same equation (plotted in Figure 9):

$$\sigma_{\tau}^2 \geq \frac{1}{2\omega_c^2 T SNR}$$

This equation takes into account distance from the transmitter and ground conductivity (since the signal strength predictions are a function of distance and conductivity) as shown in Figure 18. It also takes into account the predicted noise (in the SNR term). The accuracy is also a function of the receiver averaging time, T (5 seconds is used), and frequency, ω_c (300 kHz used).

3.2 Positioning Accuracy (LP1-350)

This equation bounding the time accuracy, converted from nanoseconds to meters, is used to provide the accuracy of each individual pseudorange. This error term is combined with the geometry of the stations through a weighted HDOP calculation to provide a bound on position accuracy estimates across the North Sea Area (see Figure 21). In calculating this, only those stations with a SNR > 7dB are used (7dB being the minimum set forth by the IEC [61]). This plot, for daytime, does not take into account any errors due to timing offsets between the various transmitters (assumed perfect synchronization), nor does it take into account any secondary variations in propagation (ASFs) as these are judged to be very small over the North Sea Area due to the limited land paths. Since the detail is difficult to see on this scale (0-100m of error), Figure 22 shows the same data plotted using a 0-20m scale.

Predicted daytime bound on R-Mode positioning accuracy using TOA bounds is very good – better than 10m accuracy in most of the North Sea Area.

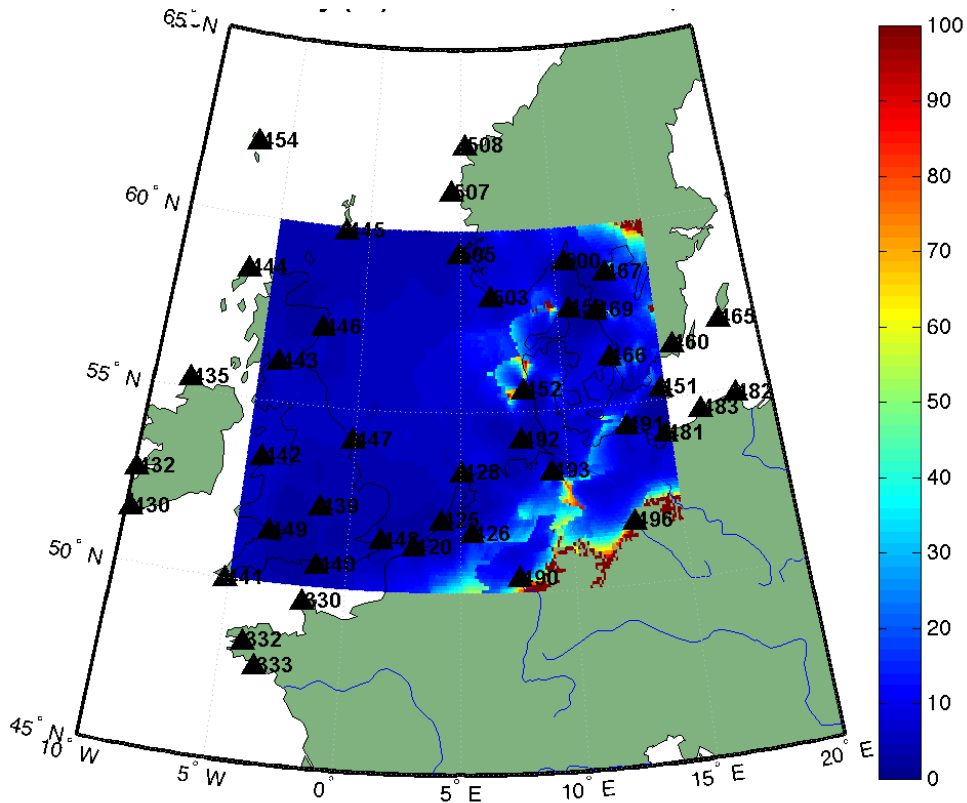


Figure 21: Daytime Predicted Positioning Accuracy (m) using 0-100m scale.

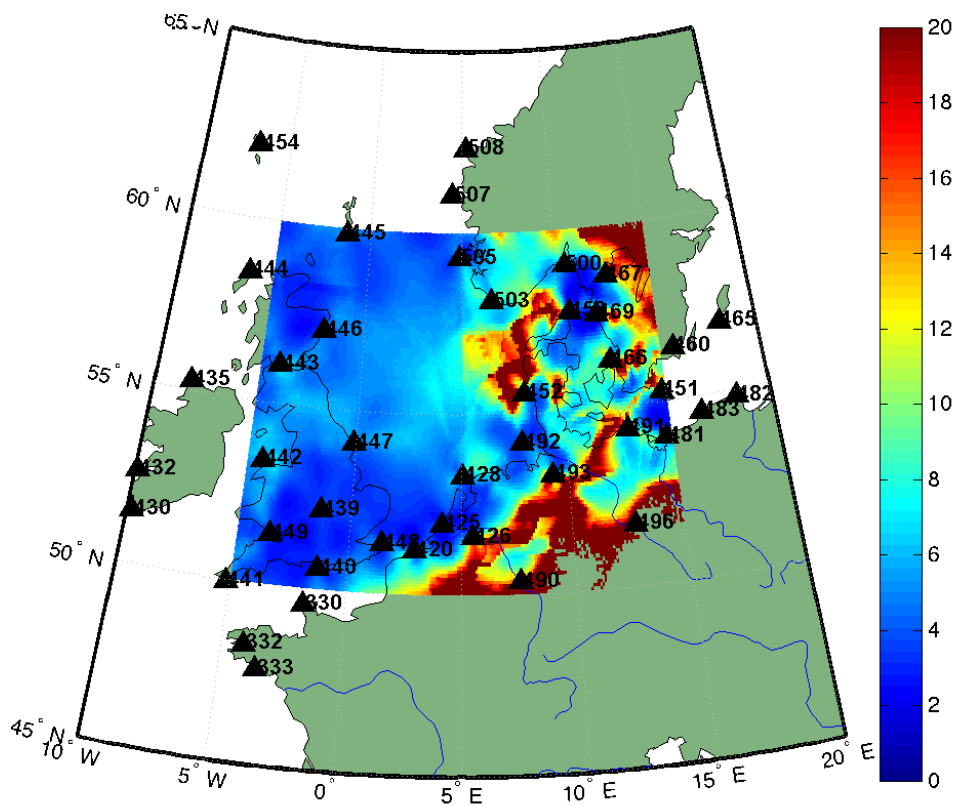


Figure 22: Daytime Predicted Positioning Accuracy (m) using 0-20m scale.

The largest impact on DGNSS R-Mode performance is sky wave interference as described in Section 2.3. In general, the sky wave interference starts building up at sunset, increases to a maximum after midnight, and then reduces back down after sunrise. The maximum night time sky wave signal strength at each location in the grid is predicted using the LFMF software tool [53], which uses the ITU-R sky wave models from [54] as described in [62]. This sky wave strength is used to impact the position solution in two ways. First, the sky wave signal strength is treated as noise and subtracted from the SNR values (a worst case of destructive interference). Second, the fade margin is calculated as the difference between the ground wave signal strength and the sky wave signal strength. This fade margin is used to calculate the additional error variance of the phase estimate as described in Section 2.3.3, which is then added to the noise variance based upon the SNR. This combined noise variance is used in the weighted HDOP solution to compute the new predicted performance grid shown in Figure 23. Since all errors over 100m are the same color in this plot, It is difficult to see the variance in some areas; Figure 24 is the same data with a 0-200m scale.

Night time R-mode performance is about a factor of 10 worse than daytime performance but still better than 100m accuracy for most of the North Sea Area.

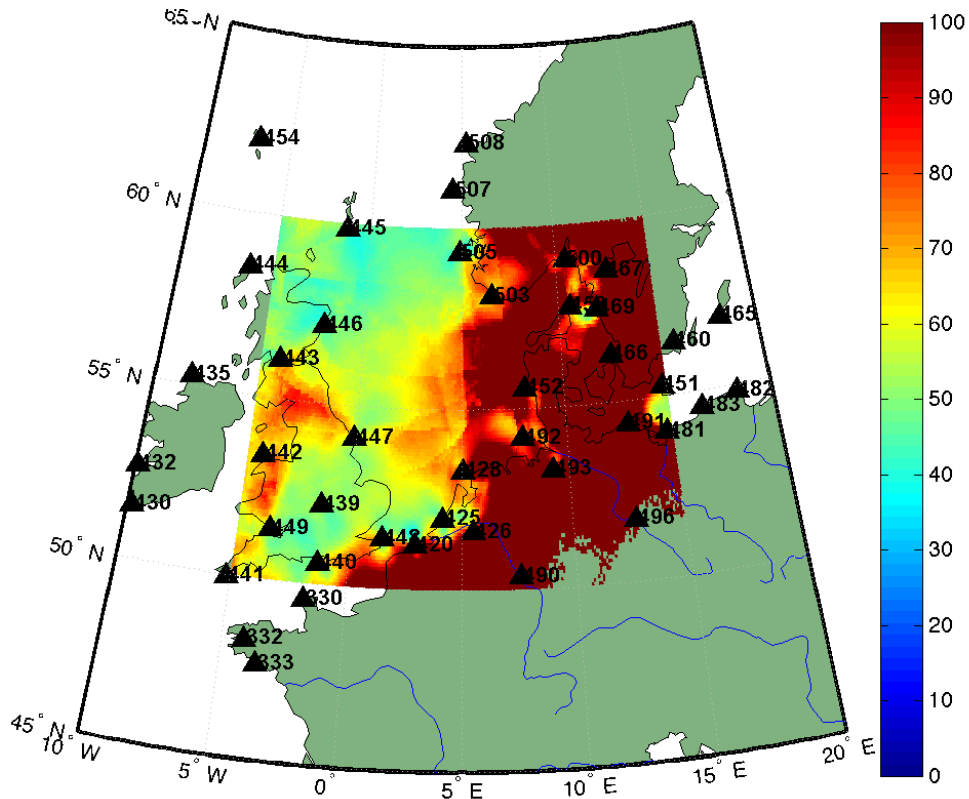


Figure 23: Predicted Positioning Accuracy (m) at night using 0-100m scale.

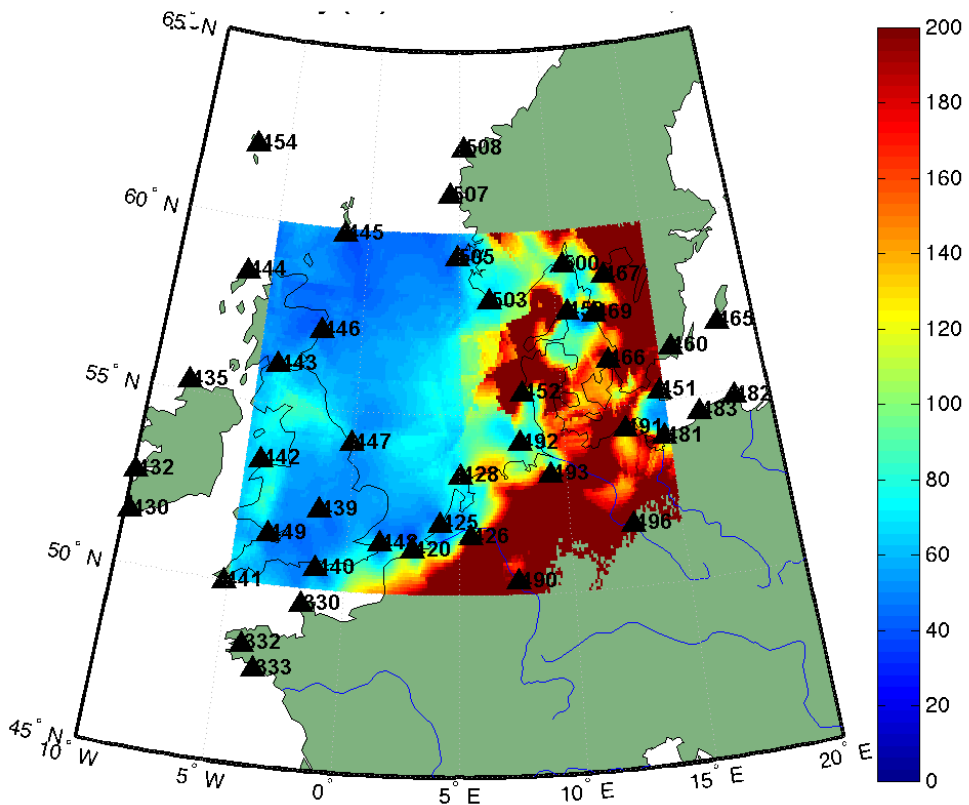


Figure 24: Predicted Positioning Accuracy (m) at night using 0-200m scale.

4 System Modifications (LP1-530)

4.1 Reference Station Modifications (LP1-360)

The subparagraphs below list the changes needed to be made to the DGNSS reference station (RTCM data formats, MSK modulator, transmitter) for each of the solutions.

4.1.1 Solution L1 (200 BPS MSK)

Solution L1 requires the following changes:

- Increase bit rate to 200 bps (this is a standard option on modulators).
- Create a new (fixed bit) RTCM message; this could either be a newly defined RTCM message or just a static message 16 [63] – if possible, a zero-one alternating sequence of the payload bits is preferred as this causes the maximum number of bit transitions.
- Install a stable clock (Rb) and a UTC time base with 50 ns synchronization accuracy each site.
- Replace the MSK modulator with one that can use the use stable clock (10MHz) and UTC sync (1PPS) signals.

If R-Mode reference stations will be used then additionally:

- Create new RTCM messages for R-Mode ranging corrections.
- Modify the Modulator to accept/use the new RTCM messages.

Figure 25 contains a block diagram of a transmitter to accomplish Solution L1.

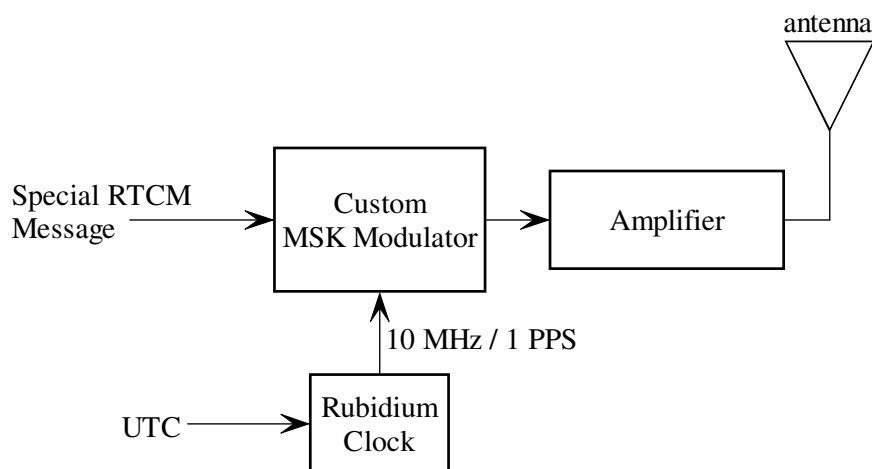


Figure 25: Transmitter for Solution L1.

4.1.2 Solution L2 (CW)

Solution L2 requires the following changes:

- Install a stable clock (Rb) and a UTC time base with 50 ns synchronization accuracy each site.
- Replace the MSK modulator with one that can use the use stable clock (10MHz) and UTC sync (1PPS) signals.

- Either modify the modulator to also generate the CW signals and combine with the MSK signal in the low-level RF feed to the transmitter or install a separate signal generator (that uses the same clock and UTC sync) and combine the two low-level RF feeds with an analog combiner.
- If the transmitter (amplifier) cannot handle a non-constant amplitude signal, then replace it with one that can.
- If the antenna/coupler cannot accommodate the wider bandwidth signal, then replace with ones that can.

If R-Mode reference stations will be used then additionally:

- Create new RTCM messages for R-Mode ranging corrections.
- Modify the Modulator to accept/use the new RTCM messages.

Figure 26 contains a block diagram of a transmitter to accomplish Solution L2.

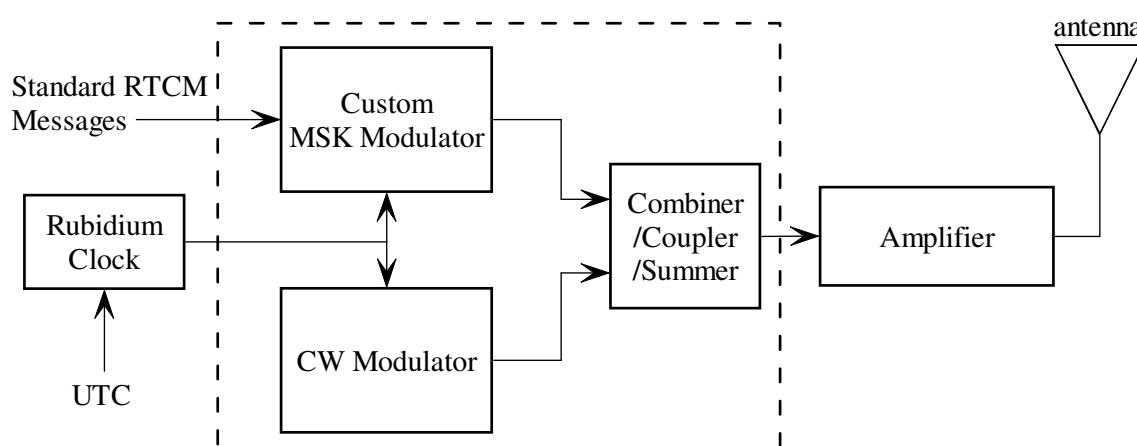


Figure 26: Transmitter for Solution L2.

4.1.3 Solution L3 (Combined)

Solution L2 requires the following changes:

- Increase bit rate to 200 bps (this is a standard option on modulators).
- Create a new (fixed bit) RTCM message; this could either be a newly defined RTCM message or just a static message 16 [63].
- Install a stable clock (Rb) and a UTC time base with 50 ns synchronization accuracy each site.
- Replace the MSK modulator with one that can use the use stable clock (10MHz) and UTC sync (1PPS) signals.
- Either modify the modulator to also generate the CW signals and combine with the MSK signal in the low-level RF feed to the transmitter or install a separate signal generator (that uses the same clock and UTC sync) and combine the two low-level RF feeds with an analog combiner.
- If the transmitter (amplifier) cannot handle a non-constant amplitude signal, then replace it with one that can.
- If the antenna/coupler cannot accommodate the wider bandwidth signal, then replace with ones that can.

If R-Mode reference stations will be used then additionally:

- Create new RTCM messages for R-Mode ranging corrections.
- Modify the Modulator to accept/use the new RTCM messages.

The block diagram of a transmitter to accomplish Solution L3 is essentially the same as the diagram shown in Figure 26 except that the unit must be able to implement the new RTCM message in addition to Standard RTCM messages.

4.2 Beacon Receiver Modifications (LP1-370)

The subsections and block diagrams below describe the changes to the beacon receiver to convert it to an R-Mode (RTCM data format, MSK demodulator) receiver for each of the three solutions. These changes will require either a new test standard or a revision to the current IEC 61108-4 standard [61].

4.2.1 Solution L1 (200 BPS MSK)

Figure 27 contains a block diagram of a receiver to implement Solution L1, which consists of the following:

- The DGNSS front end removes out of band noise and interference due to signals in the adjacent LF and AM bands. It is important that this front end not introduce time delays/phase shifts for the different DGNSS channels.
- The analog-to-digital converter (ADC) must be sufficiently fast to record the entire DGNSS band as one signal for synchronous signal processing.
- The standard MSK demodulator block estimates the transmitted bits (at 100 or 200 bps) so that the block below it (the MSK pseudorange estimator) knows how to separate the sampled data stream for the two MSK frequencies. This receiver must also be able to decode new RTCM messages in order to receive monitor site messages for pseudorange corrections and then apply these to the developed pseudoranges.
- The MSK pseudorange estimator implements several algorithms toward the goal of estimating the pseudorange: estimating the time of bit transition of the regular (random) MSK messages, estimating the pseudorange for the new (fixed) RTCM message, estimating the phase of the individual bit sinusoids, and resolving the ambiguity of this phase measurement using the bit and new message timing information. The output of this block is the estimated pseudorange and an estimate of its error variance (for weighting in the position solution).
- Finally, the pseudoranges from each DGNSS channel and their associated weights are combined into a position solution. The output should be a standard NMEA string.

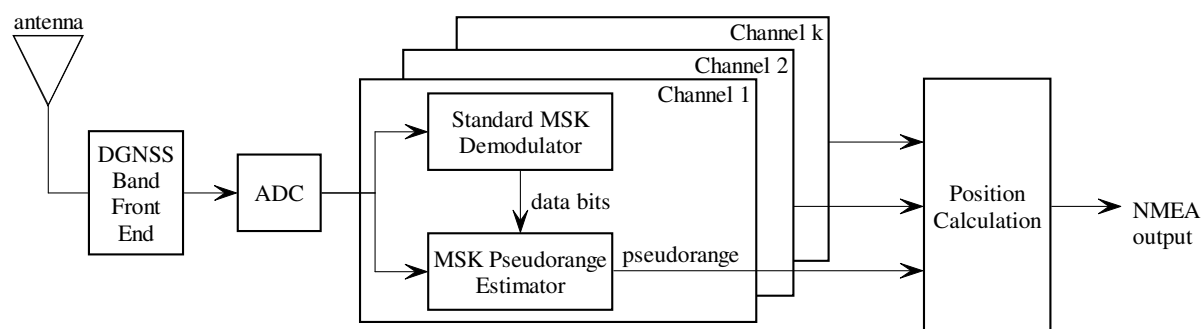


Figure 27: Receiver for Solution L1.

4.2.2 Solution L2 (CW)

Figure 28 contains a block diagram of a receiver to implement Solution L2, which consists of the following:

- The DGNSS front end removes out of band noise and interference due to signals in the adjacent LF and AM bands. It is important that this front end not introduce time delays/phase shifts for the different DGNSS channels.
- The analog-to-digital converter (ADC) must be sufficiently fast to record the entire DGNSS band as one signal for synchronous signal processing.
- The standard MSK demodulator block estimates the bit transition times so that the block below it can resolve the CW lane ambiguity. This receiver must also be able to decode new RTCM messages in order to receive monitor site messages for pseudorange corrections and then apply these to the pseudoranges
- The CW phase estimator implements standard algorithms to estimate the phases of the two transmitted CW signals.
- Ambiguity resolution is accomplished by the beat signal of these two CW signals in concert with the time of bit transition from the MSK receiver.
- Finally, the pseudoranges from each DGNSS channel and their associated weights are combined into a position solution. The output should be a standard NMEA string.

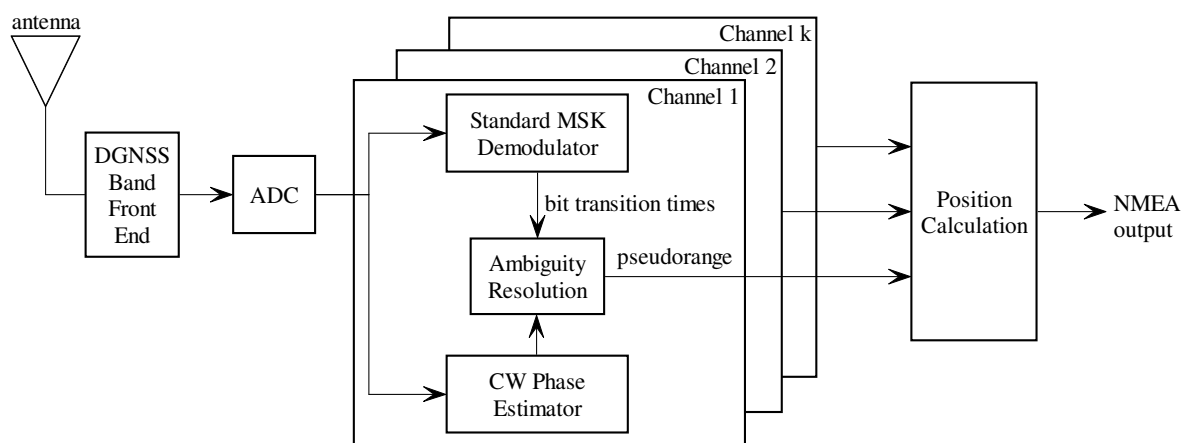


Figure 28: Receiver for Solution L2.

4.2.3 Solution L3 (combined)

Figure 29 of a receiver to implement Solution L3, which consists of the following:

- The DGNSS front end removes out of band noise and interference due to signals in the adjacent LF and AM bands. It is important that this front end not introduce time delays/phase shifts for the different DGNSS channels.
- The analog-to-digital converter (ADC) must be sufficiently fast to record the entire DGNSS band as one signal for synchronous signal processing.
- The standard MSK demodulator block decodes any new RTCM messages in order to receive monitor site messages for pseudorange corrections and then apply these to the developed pseudoranges.
- The MSK pseudorange estimator block estimates the pseudorange for the occasionally occurring new (fixed) RTCM message.

- The CW phase estimator implements the standard algorithm for the phase of the one transmitted CW signal.
- The ambiguity resolution is accomplished by selecting the CW lane to match the pseudorange estimated from the fixed RTCM message.
- Finally, the pseudoranges from each DGNSS channel and their associated weights are combined into a position solution. The output should be a standard NMEA string.

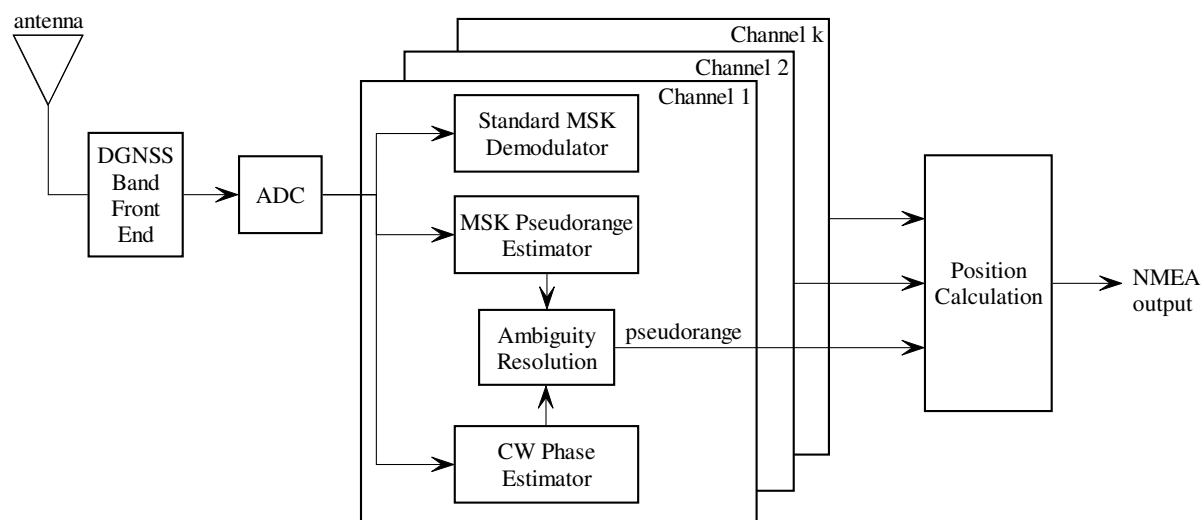


Figure 29: Receiver for Solution L3.

4.3 Clock Specification (LP1-380)

There is a trade-off between accuracy, cost, complexity, and coverage area. Probably the best recommendation would be to install Rb clocks at the DGNSS sites to provide the short-term signal stability and use a UTC time base to synchronize the clocks. This would provide R-Mode positioning coverage throughout the area at a level of accuracy limited by the clock synchronization accuracy (50-100ns). For Harbor Entrance and Approach (HEA) areas, reference sites would be needed to enable higher accuracy. The other option (and maybe the easiest option for test bed use) would be to use a GPS timing receiver as the UTC reference, accepting the limited holdover time in the loss of GPS. Caesium clocks would provide much longer holdover time, but are an order of magnitude more expensive than Rb clocks.

Minimum frequency accuracy: 5×10^{-11}

Minimum Stability: 1×10^{-10} .

Minimum UTC synch accuracy: 50 ns.

4.4 Potential Improvements (LP1-395)

There are several additional avenues that could be pursued in the future to improve the performance of the solutions presented. First, if a sky wave reducing antenna (one that attenuates high elevation angle signals) could be found, then the use of such an antenna could increase the night time coverage area considerably. Second, if a directional antenna

(such as one formed from H-field crossed-loops [64]) was used, then a bearing could be estimated for each received signal. This bearing could then be incorporated into the position solution algorithm along with the pseudoranges. This could potentially improve the accuracy, and would also improve the coverage area by reducing the number of beacon stations needed. Third, ASF maps could be measured and made available to the user receiver to eliminate the propagation errors. And finally, as already mentioned, reference sites could be used to calculate and transmit R-Mode ranging corrections to improve performance in the area around the reference station.

5 Test Bed Concept (LP1-540)

The following two subsections provide descriptions of two concepts for testing the DGNSS R-mode in a real test bed, first in the short term (ACCSEAS) and second in the longer term.

5.1 Development of concept for testing R-Mode in a field trial (LP1-400)

The ACCSEAS Test Bed is only chartered through early 2015; this limits what can be included as part of the test bed. However, even a limited test can serve as a proof-of-concept and provide a basis for further work. The following is what the authors believe is something that can be accomplished within the timeframe of the ACCSEAS Test Bed and still be meaningful as an R-Mode field trial:

- Install a single R-Mode transmitter at one site.
- Build a single mobile R-Mode receiver to be installed on a vessel of opportunity.
- Build and install a fixed R-Mode receiver to act as a monitor site.

5.1.1 Transmitter

A single DGNSS site would need to be chosen. There are several options for this. First, the planned facility at Ijmuiden Phare might be used (see Figure 30). The construction of the antenna tower has not started yet, so this might not be available within the required timeframe. A temporary antenna could be used for the test, but might not be capable of the range desired. A second option would be to use one of the Dutch operational sites (such as at Holland Hook). This would require approval for use of the operational site. A third option would be to use the German operational site at Helgoland.



Figure 30: Ijmuiden site (black triangle) with 200 km range ring in yellow and 100 km range ring in red.

Regardless of which transmitter *location* is chosen, the transmitter should have a modulator such as the Flexibilis modulator (see Figure 31) used in the Finnish Time Transfer testing [13] that can be synchronized to UTC (both carrier and bit clock) and that can transmit a custom RTCM message. The transmitter would be set to transmit just the custom message and no “real” messages (RTCM Type 9’s). Employing this fixed signal would allow us to test L1 and partially test L2 (while setting all of the bits to zero or one generates a single CW signal, there would only be the one signal, not at the intended frequency, and the MSK would not be present).



Figure 31: Flexibilis DGNSS Modulator.

5.1.2 Mobile Receiver

At least one mobile receiver would be needed. This R-Mode receiver needs to have the capability of measuring the pseudorange from the R-Mode transmitter. The R-mode receiver should also accept NMEA sentences from a DGNSS receiver in order to estimate the error in the pseudorange in real time. This data on pseudoranges and errors should be logged along with position and time for later analysis.

5.1.3 Monitor Receiver

An additional receiver is needed to act as a fixed monitor site. This R-Mode receiver needs to have the capability of measuring the pseudorange from the R-Mode transmitter. The R-mode receiver should also accept NMEA sentences from a DGNSS receiver in order to estimate the error in the pseudorange in real time. This data on pseudoranges and errors should be logged along with position and time for later analysis. This monitor site should be located about 100km from the transmitter. This will enable study of the impacts of sky wave on the pseudorange estimation error.

5.2 Field test concept study (LP1-410)

If the timeline is extended into the future more, then a better test bed for the North Sea Area can be designed and implemented. This future German R-Mode test bed could be configured to assess the performance of the recommended solution set (using CW signals) as well as full positioning by using multiple R-Mode transmitters.

5.2.1 Transmitter Locations

In order to do R-Mode positioning at least three R-Mode transmitters are needed. Looking at the existing DGNSS transmitter locations a good geographic location for the test bed would be in the Helgoland Bight. This is also the entrance to Hamburg, which is the third busiest port in Europe, so is a critical area. The best case for this area would be to use five DGNSS stations as shown in Figure 32 as this provides excellent predicted positioning performance in an area within 150km of the approaches to Hamburg (red circle in Figure 32). Adding just one of the two non-German stations (see Figure 33 and Figure 34) does not improve the predicted position performance much over the case of just using the three German stations (see Figure 35). If the test bed needed to be limited to 4 stations then dropping Gross Mohrdorf would be the best option (see Figure 36).

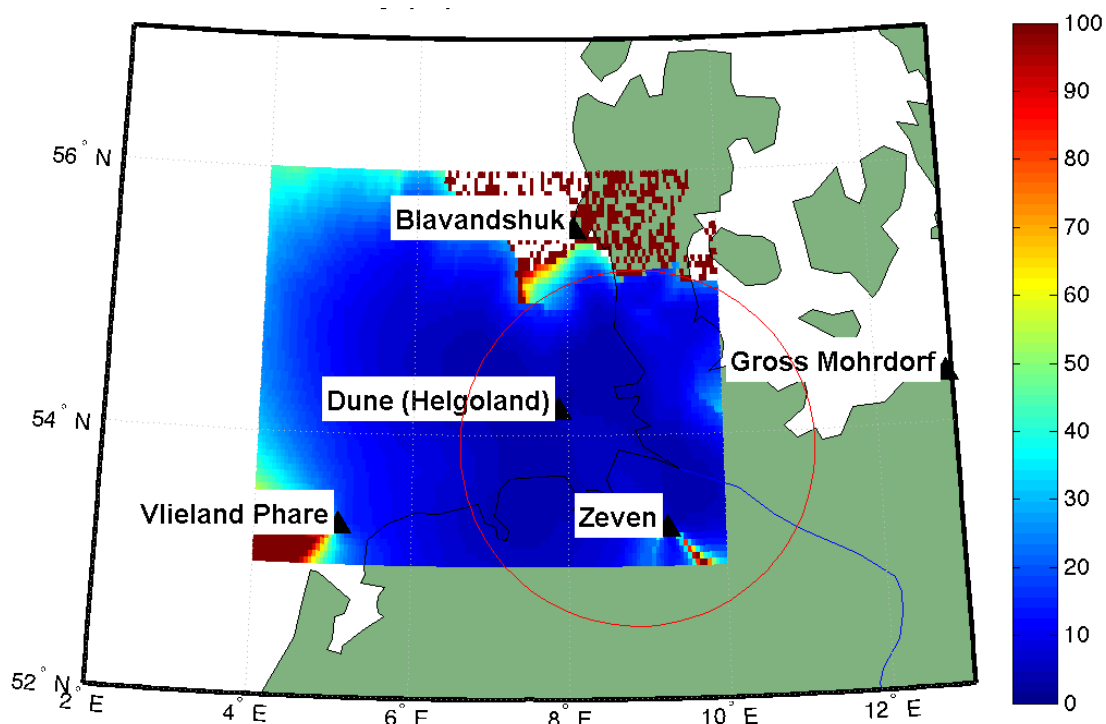


Figure 32: Test Bed HDOP for three German Stations plus Netherlands and Denmark.

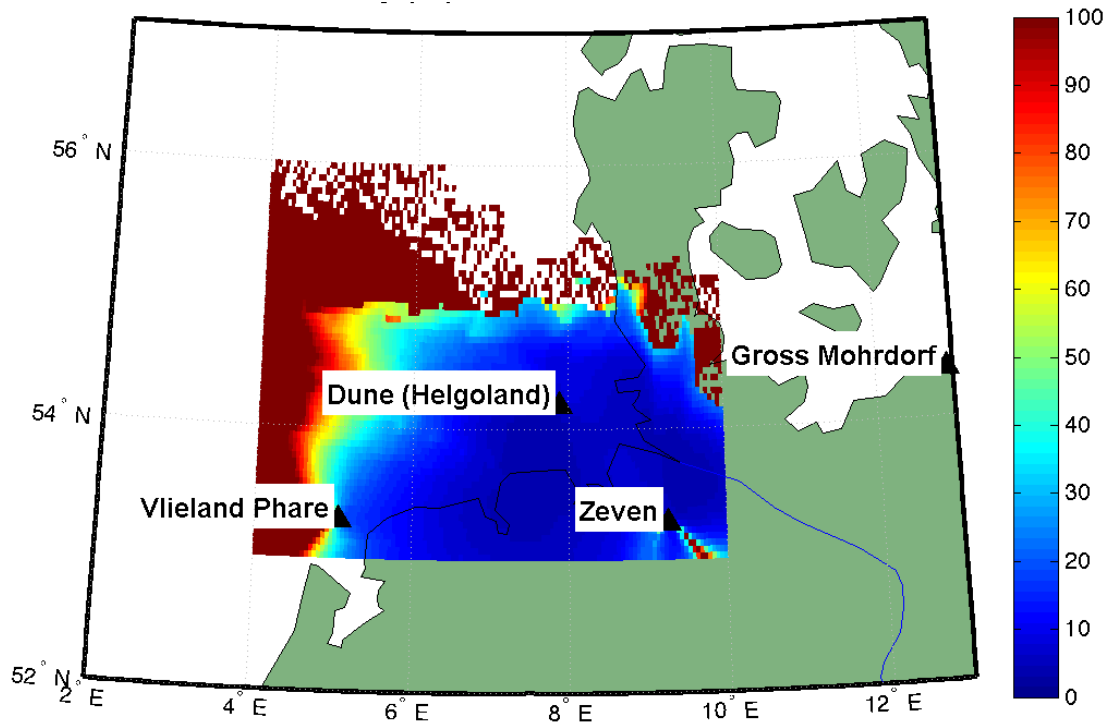


Figure 33: Test Bed HDOP for three German Stations plus Netherlands.

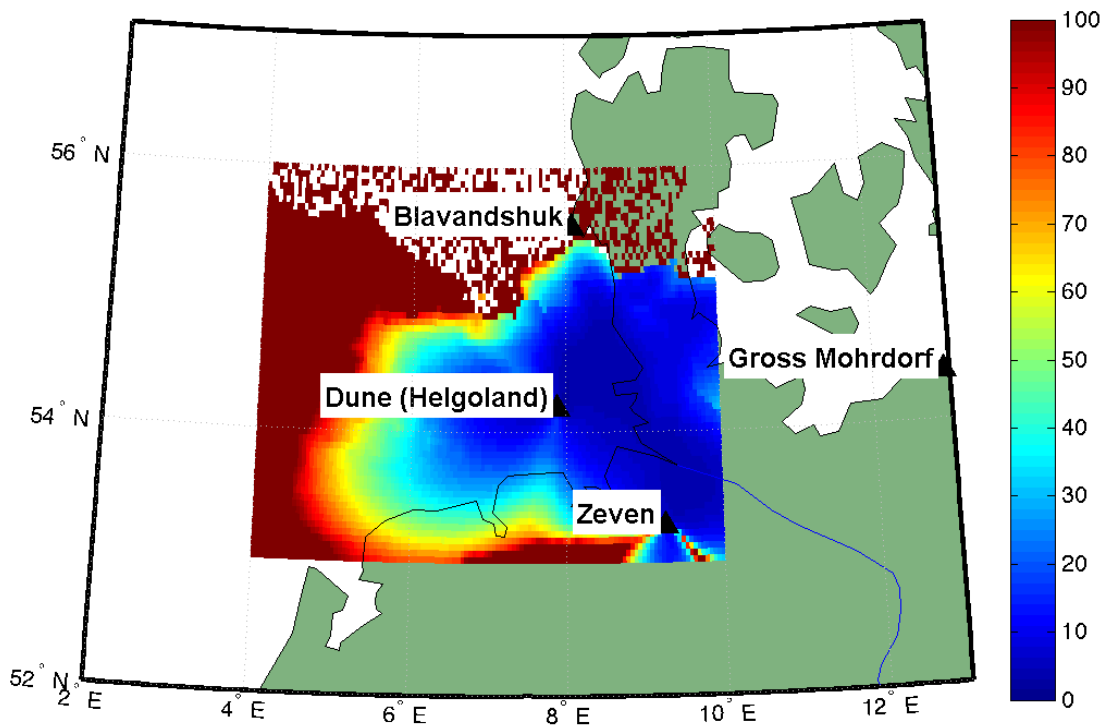


Figure 34: Test Bed HDOP for three German Stations plus Denmark.

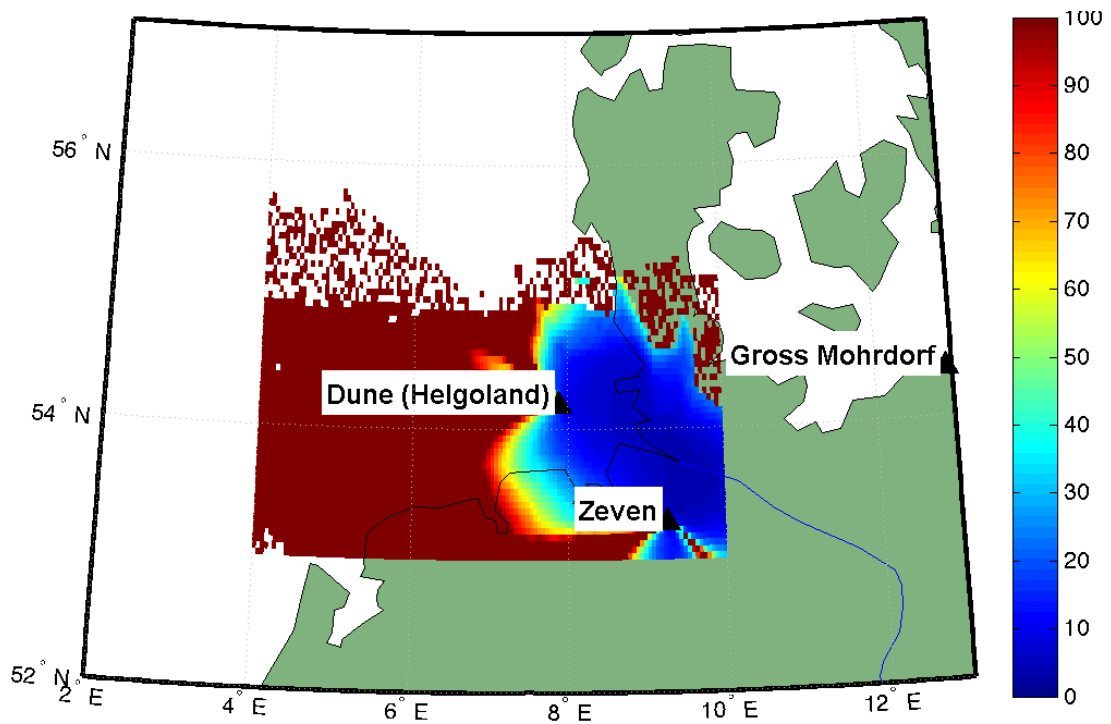


Figure 35: Test bed HDOP for three German Stations.

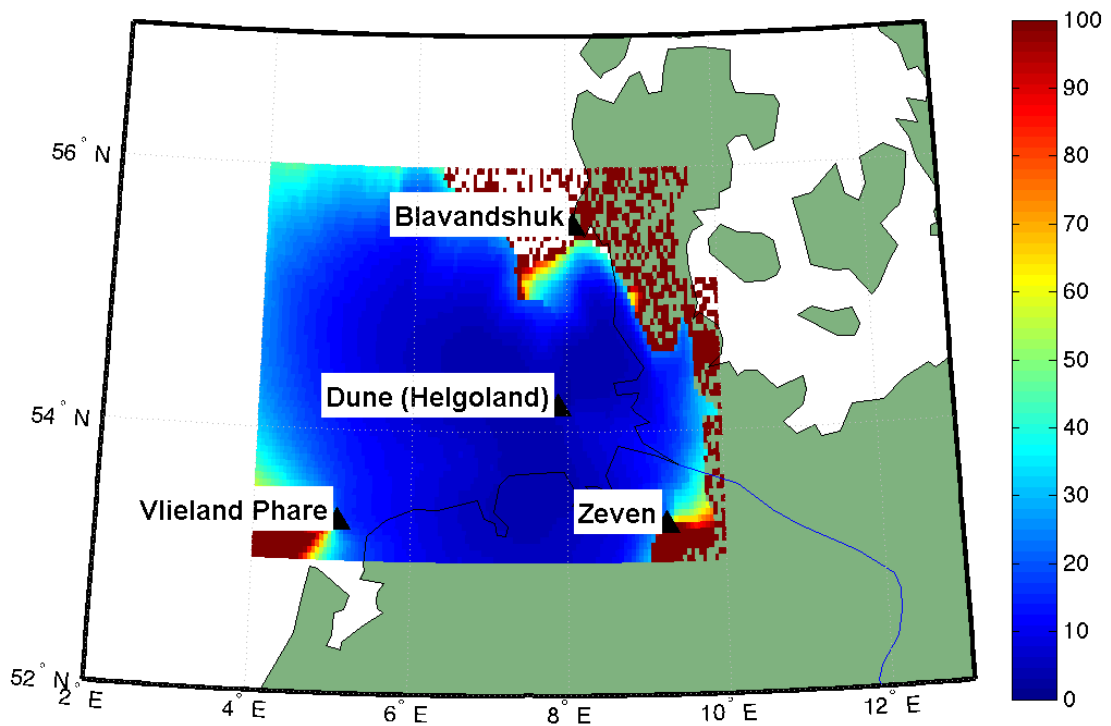


Figure 36: Test Bed HDOP for two German Stations plus Netherlands and Denmark.

5.3 R-mode Receiver Concept (LP1-420)

As depicted in Figure 37 the full R-Mode prototype receiver is envisioned as an “all-in-view” system, receiving and processing as many R-Mode signals as possible (shown in the figure as channels 1 through k) and using them all in the position solution. In this model each channel consists of several operations:

- Demodulating the individual MSK transmissions for DGNSS and/or R-Mode correction data. The R-Mode correction data will be employed by the position calculation algorithm.
- Appropriate signal processing (estimation algorithms) to estimate a pseudorange from the received signal. Depending upon the solution utilized (L1, L2, or L3), this is a combination of MSK bit transition tracking, CW phase tracking, and/or ambiguity resolution.
- An assessment of the quality of the derived pseudorange for each channel; specifically an assessment of the variance of the pseudorange error and, perhaps, whether or not the signal is corrupted by skywave. Accurate assessment of this quality is required for a high performance position solution and is employed as part of the position calculation itself (pseudoranges with larger error variances are down-weighted in the solution).

The proposed receiver structure shows a common RF front end and ADC as an accurate position solution depends upon keeping the individual R-Mode channels in time synchronization. Further, the receiver’s internal clock used to drive the ADC (shown explicitly in this block diagram) needs to be uniform over the observation time of the receiver with good frequency stability so that the individual channels can be separated.

Once a sufficient number of pseudoranges are estimated (at least three for latitude, longitude, and receiver clock offset computation, but more are better), a weighted least squares position calculation is implemented. The resulting position, in the WGS 84 datum, would be output from the receiver. Additional output information should include the list of stations employed in the solution, the quality of their measurements, and the receiving geometry (HDOP).

It is envisioned that prototype receivers would be constructed using software defined radio peripherals (e.g. USRP-like front ends or fast ADC cards) with the signal processing being done in a computational software environment (e.g. MATLAB or equivalent). Production receivers would leverage FPGA implementations.

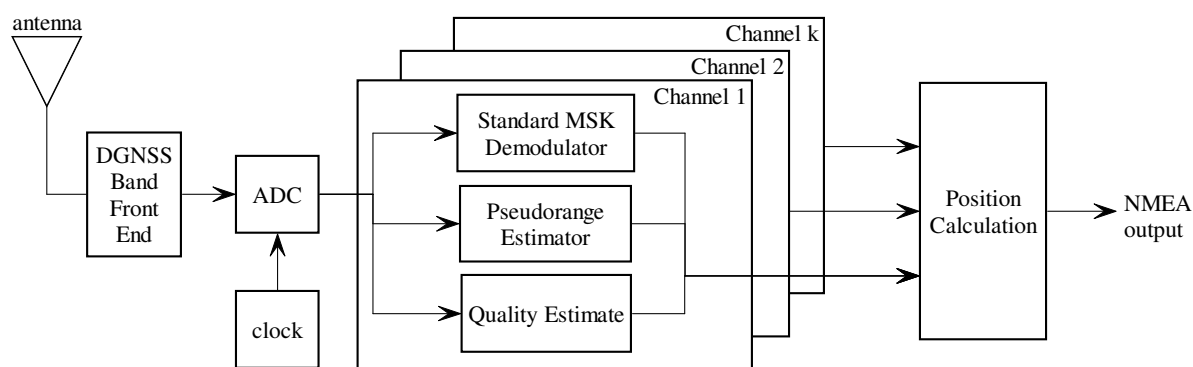


Figure 37: All-in-view R-Mode receiver.

7 References

- [1] "The e-Navigation Architecture - the Shore-based Perspective, 2nd Edition DRAFT," International Association of Marine Aids to Navigation and Lighthouse Authorities (IALA), Saint Germain en Laye, France, IALA Recommendation e-NAV-140, December 2013.
- [2] "the IALA Common Shore-based System Architecture (CSSA) - DRAFT," International Association of Marine Aids to Navigation and Lighthouse Authorities (IALA), Saint Germain en Laye, France, IALA Recommendation e-NAV-???, December 2013.
- [3] T. Porathe, "ACCSEAS Baseline and Priorities Report," 2013.
- [4] G. W. Johnson, P. F. Swaszek, R. J. Hartnett, C. Oates, and M. Wiggins, "Beacon-Loran Integrated Navigation Concept (BLINC): an Integrated Medium Frequency Ranging System," presented at the Institute of Navigation GNSS 2007, Fort Worth, TX, 2007.
- [5] P. Swaszek, "DGPS-based trilateration receiver," USDOT Federal Highways Administration SBIR Phase I Final Report, November 2008.
- [6] P. F. Swaszek, R. J. Hartnett, and G. W. Johnson, "Ranging/Timing Off of the NDGPS Signal: Potential Performance," presented at the Institute of Navigation International Technical Meeting, Newport Beach, CA, 2012.
- [7] P. F. Swaszek, G. W. Johnson, R. J. Hartnett, A. B. Cleveland, and S. Barr, "Ranging/Timing Using the NDGPS Signal," in *ION GNSS 2012*, Nashville, TN, 2012.
- [8] J. A. McEllroy, "Navigation using Signals of Opportunity in the AM Transmission Band," MS, Aeronautics and Astronautics, Air Force Institute of Technology, Dayton, OH, 2006.
- [9] T. A. Webb, P. D. Groves, P. A. Cross, R. J. Mason, and J. H. Harrison, "A New Differential Positioning Method using Modulation Correlation of Signals of Opportunity," in *Position Location and Navigation Symposium (PLANS), 2010 IEEE/ION*, 2010, pp. 972-981.
- [10] T. D. Hall, C. C. Counselman, and P. Misra, "Instantaneous Radiolocation Using AM Broadcast Signals," in *Institute of Navigation, National Technical Meeting*, Long Beach, CA, 2001.
- [11] P. J. Duffett-Smith and G. Woan, "The CURSOR Radio Navigation and Tracking System," *The Journal of Navigation*, vol. 45, pp. 157-165, 1992.
- [12] T. D. Hall, "Radiolocation Using AM Broadcast Signals," Massachusetts Institute of Technology, 2002.
- [13] K. Heikonen, "Test Results on Accurate Time Transfer via DGNSS MF Transmissions," Finnish Transport Administration, Input Paper e-NAV10/8/13, 2010.
- [14] R. Mutanen, "Accurate Time Transfer via DGPS Stations," VTT Technical Research Centre of Finland, 16 Mar, PowerPoint Presentation, unpublished.
- [15] A. J. Fisher, "Digital signal processing of Decca Navigator radionavigation signals," *Radar, Sonar and Navigation, IEE Proceedings -*, vol. 142, pp. 71-80, 1995.
- [16] P. Enge, D. Young, and B. Butler, "Two-tone Diversity to Extend the Range of DGPS Radiobeacons," *Navigation: Journal of the Institute of Navigation*, vol. 45, pp. 161 - 171, Fall 1998.
- [17] S. Pasupathy, "Minimum Shift Keying: A Spectrally Efficient Modulation," *IEEE Communications Magazine*, vol. 17, pp. 14-22, 1979.

- [18] F. Amoroso, "Pulse and Spectrum Manipulation in the Minimum (Frequency) Shift Keying (MSK) Format," *Communications, IEEE Transactions on [legacy, pre - 1988]*, vol. 24, pp. 381-384, 1976.
- [19] R. W. D. Booth, "An Illustration of the MAP Estimation Method For Deriving Closed-Loop Phase Tracking Topologies: The MSK Signal Structure," *IEEE Transactions on Communications*, August 1980.
- [20] P. Galko and S. Pasupathy, "Linear Receivers for Correlatively Coded MSK," *IEEE Transactions on Communications*, vol. COM-33, pp. 338-347, April 1985 1985.
- [21] C. Colavolpe and R. Raheli, "Noncoherent Sequence Detection of CPM," *Electronics Letters*, vol. 34, p. 2, February 1998.
- [22] T. Masamura, S. Samejima, Y. Morihira, and H. Fuketa, "Differential Detection of MSK with Nonredundant Error Correction," *Communications, IEEE Transactions on*, vol. 27, pp. 912-918, 1979.
- [23] G. K. Kaleh, "A differentially coherent receiver for minimum shift keying signal," *Selected Areas in Communications, IEEE Journal on*, vol. 7, pp. 99-106, 1989.
- [24] H. Leib and S. Pasupathy, "Noncoherent block demodulation of MSK with inherent and enhanced encoding," *Communications, IEEE Transactions on*, vol. 40, pp. 1430-1441, 1992.
- [25] B. Li, "Decision feedback detection of minimum shift keying," *Communications, IEEE Transactions on*, vol. 44, pp. 1073-1076, 1996.
- [26] S. Junna, "A new software demodulation method for MSK signal based on phase information," in *Systems and Control in Aerospace and Astronautics, 2006. ISSCAA 2006. 1st International Symposium on*, 2006, pp. 3 pp.-830.
- [27] R. de Buda, "Coherent Demodulation of Frequency-Shift Keying With Low Deviation Ratio," *IEEE Transactions on Communications*, pp. 429-435, June 1972.
- [28] R. E. Ziemer and C. Ryan, "Minimum-shift keyed modem implementations for high data rates," *Communications Magazine, IEEE*, vol. 21, pp. 28-37, 1983.
- [29] A. N. D'Andrea, U. Mengali, and R. Reggiannini, "A Digital Approach to Clock Recovery in Generalized Minimum Shift Keying," *IEEE Transactions on Vehicular Technology*, vol. 39, p. 8, August 1990.
- [30] C. N. Georghiades and M. Moeneclaey, "Sequence Estimation and Synchronization from Nonsynchronized Samples," *IEEE Transactions on Information Theory*, November 1991.
- [31] R. Mehlan, Y.-E. Chen, and H. Meyr, "A Fully Digital Feedforward MSK Demodulator with Joint Frequency Offset and Symbol Timing Estimation for Burst Mode Mobile Radio," *IEEE Transactions on Vehicular Technology*, vol. 42, p. 10, November 1993.
- [32] U. Lambrette and H. Meyr, "Two Timing Recovery Algorithms For MSK," in *IEEE ICC '04, New Orleans, LA, 1994*.
- [33] K. H. Chang and C. N. Georghiades, "Joint Maximum-Likelihood Timing and Data Estimation for MSK Signals from Matched-Filter Samples," in *IEEE ICC '04, New Orleans, LA, 1994*.
- [34] A. N. D'Andrea, U. Mengali, and M. Morelli, "Symbol timing estimation with CPM modulation," *Communications, IEEE Transactions on*, vol. 44, pp. 1362-1372, 1996.
- [35] M. Morelli and G. M. Vitetta, "Joint Phase and Timing Recovery for MSK-Type Signals," *IEEE Transactions on Communications*, vol. 48, December 2000.
- [36] M. Morelli and U. Mengali, "Joint Frequency and Timing Recovery for MSK-Type Modulation," *IEEE Transactions on Communications*, vol. 47, p. 9, June 1999.

- [37] Y.-C. Wu and T.-S. Ng, "Symbol Timing Recovery for Generalized Minimum Shift Keying Modulations in Software Radio Receiver," in *Global Telecommunications Conference (GLOBECOM '01)*, 2001, pp. 3302-3305.
- [38] Y. Wu and E. Serpedin, "Design and Analysis of Feedforward Symbol Timing Estimators Based on the Conditional Maximum Likelihood Principle," *IEEE Transactions on Signal Processing*, may 2005.
- [39] U. Mengali and A. N. D'Andrea, *Synchronization Techniques for Digital Receivers*: Springer, 1997.
- [40] H. Meyr, M. Moeneclaey, and S. A. Fechtel, *Digital Communication Receivers, Synchronization, Channel Estimation, and Signal Processing*: Wiley, 1997.
- [41] H. Meyr and G. Ascheid, *Digital Communication Receivers: Synchronization in Digital Communication Volume I, Phase-, Frequency-Locked Loops, and Amplitude Control*, 1990.
- [42] S. M. Kay, *Fundamentals of Statistical Signal Processing, Volume I: Estimation Theory*: Prentice Hall, 1993.
- [43] A. N. D'Andrea, U. Mengali, and R. Reggiannini, "The Modified Cramer-Rao Bound And its Application to Synchronization Problems," *IEEE Transactions on Communications*, Feb/Mar/Apr 1994.
- [44] F. Gini, R. Reggiannini, and U. Mengali, "The Modified Cramér-Rao Bound in Vector Parameter Estimation," *IEEE Transactions on Communications*, January 1998.
- [45] J. F. Kasper and C. E. Hutchinson, "The Omega navigation system--An overview," *Communications Society Magazine, IEEE*, vol. 16, pp. 23-35, 1978.
- [46] A. D. Whalen, *Detection of Signals in Noise*. San Diego: Academic Press, 1971.
- [47] D. Rife and R. R. Boorstyn, "Single tone parameter estimation from discrete-time observations," *Information Theory, IEEE Transactions on*, vol. 20, pp. 591-598, 1974.
- [48] S. Sezginer, "Symbol Synchronization for MSK Signals based on Matched Filtering," MSEE MSEE, Graduate School of Natural and Applied Sciences, Middle East Technical University, 2003.
- [49] P. Swaszek, G. Johnson, R. Hartnett, C. Oates, and M. Wiggins, "Methods for Developing ASF Grids for Harbor Entrance and Approach," presented at the 35th Annual Technical Symposium, International Loran Association, Groton, CT, 2006.
- [50] P. Williams and D. Last, "Mapping the ASFs of the Northwest European Loran-C System," in *28th Annual Convention and Technical Symposium, International Loran Association*, 1999.
- [51] K. Dykstra, D. Last, and P. Williams, "Propagation of Loran-C Signals in Irregular Terrain- Modeling and Measurements, Part II: Measurement," in *29th Annual Convention and Technical Symposium, International Loran Association*, Washington, DC, 2000.
- [52] *ITU-R Handbook on the Ionosphere and its Effects on Radiowave Propagation*. Geneva: ITU-R, 1998.
- [53] N. DeMinco and J. Geikas, "User Manual for Low and Medium Frequency Propagation Model," July 1998.
- [54] "Prediction of Sky-wave Field Strength at Frequencies Between About 150 and 1700 kHz," International Telecommunication Union - Radiocommunication Sector, Geneva, ITU Standard ITU-R P.1147-4, 2007.
- [55] P. Williams, C. Hargreaves, D. Last, and N. Ward, "eLoran in the UK: Leading the Way," presented at the ION 2013 Pacific PNT Meeting, Honolulu, HI, 2013.

- [56] P. Brunavs, "Report on Investigation of Effects of Inhomogeneous and Irregular Terrain on the Groundwave Propagation at 100 kHz," Atlantic Oceanographic Laboratory, Bedford Institute, Dartmouth, N.S. CA1976.
- [57] A. Thönnies and M. Hoppe, "Creating Software for Computer-aided Frequency Planning in DGNSS Band," *Seezeichenversuchsfeld*, August 1998.
- [58] "World Atlas of Ground Conductivities," International Telecommunications Union Radiocommunication Assembly (ITU-R), Geneva, Recommendation ITU-R M.832-2, 1999.
- [59] A. Grant, "Availability, continuity, and selection of maritime DGNSS radiobeacons," Doctor of Philosophy, School of Informatics, University of Wales, Bangor, UK, 2002.
- [60] "Recommendation ITU-R P.372-8: Radio Noise," ITU, Geneva, International Standard P.372-8, 2003.
- [61] "Maritime Navigation and Radiocommunication Equipment and Systems - Global Navigation Satellite Systems (GNSS) - Part 4: Shipborne DGPS and DGLONASS Maritime Radio Beacon Receiver Equipment - Performance Requirements, Methods of testing and Required Test Results," International Electrotechnical Commission, International Standard IEC 61108-4, 2004.
- [62] N. DeMinco, "Propagation Prediction Techniques and Antenna Modeling (150 to 1705 kHz) for Intelligent Transportation Systems (ITS) Broadcast Applications," *IEEE Antennas and Propagation Magazine*, vol. 42, p. 26, August 2000.
- [63] "Differential GNSS (Global Navigation Satellite Systems) Service - Version 2.3," Radio Technical Commission for Maritime Services (RTCM) Special Committee No. 104, Alexandria, VA, Standard RTCM 10402.3, 20 August 2001.
- [64] L. Hartshorn, P. Swaszek, G. Johnson, K. Gross, R. Hartnett, C. Oates, *et al.*, "DGPS Directional Signal Strength Meter," presented at the Institute of Navigation Annual Meeting, Cambridge, MA, 2005.